Swiss Soft Days

18th Edition

Zurich, 30.3.2016

How/when to get there:

Welcome to the 18th Edition of the Swiss Soft Days!

The conference venue is in the main building of ETH (HG D 5.2) located in Rämistrasse 101.

Address
ETH Zurich
Zentrum

Rämistrasse 101
8092 Zurich
Switzerland

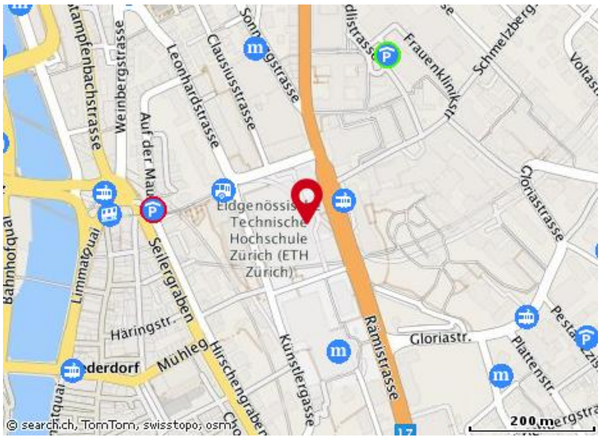

Travelling by public transport from Zurich Central Station:

From the "Bahnhofstrasse/HB" stop: Tram no. 6 (towards the Zoo) as far as the "ETH/Universitätsspital" stop. Journey time: approx. 6 minutes.

From the "Bahnhofplatz/HB" stop: Tram no. 10 (towards the Airport or Oerlikon station) as far as the "ETH/Universitätsspital" stop or Tram no. 3 (towards Klusplatz) as far as the "Central" stop (1 stop), from "Central" by Polybahn (departs every three minutes) to the Polyterrasse. Journey time: approx. 8 minutes.

You will require a ticket that is valid for zone 110 (city of Zurich).

Directions on how to reach the ETH main building can be found at the bottom of the map on the left. The venue can also be reached on foot within 10 to 15 minutes. The conference room is located on the mezzanine ground floor (D level) of the building and there will be signs directing to it.

The scientific program (see next page) will start at 10:15am. Registration and a welcome coffee will be available from 09:30am sponsored by Instrumat.

The program features two keynote speakers (Prof. Eric M. Furst, University of Delaware and Dr. Armin W. Knoll, IBM Research-Zurich) and 12 short talks of 15 minutes each including questions. Time for additional discussions will available during the breaks and the poster session.

The poster session will take place between 12:00 and 13:30 in front of the lecture room, together with lunch, in the foyer in front of the lecture room. Poster boards and pins will be provided.

If you have any questions do not hesitate to contact us at lucio.isa@mat.ethz.ch

Have a happy meeting!

The local organizers

Lucio Isa

Peter Fischer

Jan Vermant

Program

09:30-10:15: Welcome Coffee/Registration

10:15-11:00: *"Directing colloidal self-assembly using toggled fields"* (Eric M. Furst)

<u>Session 1: Rheology</u> (Chair: Peter Fischer)

11:00-11:15: *"Shear rheology of polystyrene melts and solutions with the same number of entanglements"* (S. Costanzo)

11:15-11:30: *"Viscoelastic spectrum of sheared model hard sphere and interpenetrable soft colloidal glasses"* (A. R. Jacob)

11:30-11:40: *"Soft apple cells suspensions: How does structural parameters and continuous phase impact rheological behaviour?"* (C. Leverrier)

11:45-12:00: *"Aggregation kinetic of magneto-rheological fluids under confinement"* (K. Shahrivar)

12:00-13:30: Lunch + Poster Session

13:30-14:15: *"Nanofluidic Brownian Motors"* (Armin W. Knoll)

<u>Session 2: Particle assembly and manipulation</u> (Chair: Jan Vermant)

14:15-14:30: *"Dielectrophoretic Tweezers"* (A. F. Demirörs)

14:30-14:45: *"Insights into the mechanisms of capillary assembly"* (S. Ni)

14:45-15:00: *"Charge spectrometry on single macromolecules in solution"* (F. Ruggeri)

15:00-15:15: *"Contact line around spherical particles trapped at anisotropic fluid interfaces"* (N. Senbil)

15:15-16:00: Afternoon Coffee + Poster Session

<u>Session 3: Macromolecular materials</u> (Chair: Kaori Sugihara)

16:00-16:15: *"Biomimetic engineering of polymersome membranes for stimuli triggered activity of nanoreactors"* (T. Einfalt)

16:15-16:30: *"Aligned crystallites in gyroid-forming triblock copolymer films"* (I. Gunkel)

16:30-16:45: *"Development of membrane mechanosensor"* (R. D. Ortuso)

16:45-17:00: *"Cis-to-trans isomerization of C-C-double bond by single molecule force spectroscopy"* (M. Radiom)

Invited Lecture

Directing colloidal self-assembly using toggled fields

Eric M. Furst[1]

[1] *University of Delaware, 150 Academy St., Newark, DE 19716 USA.*

Suspensions of polarizable colloids are expected to form crystalline equilibrium phases when exposed to a steady, uniform field. Such self-assembly can be harnessed as a bottom-up process to create new photonic and phononic materials. However, in a strong field, colloids become localized and the field-induced phase transition arrests; the suspension persists indefinitely as a kinetically trapped, percolated structure.

We show that by toggling the applied field on and off the initial gel-like network structure coarsens diffusively for a time that scales exponentially with frequency. Beyond this break through time, suspensions cease diffusive coarsening and undergo an apparent Rayleigh-Plateau instability. The magnetic field drives suspensions to condense into dispersed, domains of body-centered tetragonal crystals. Within these domains the crystalline order depends on the pulse frequency. Because the scaling of the break through time with respect to frequency is exponential, the steady state limit corresponding to an infinite pulse frequency is kinetically arrested and the equilibrium state is unreachable.

These experiments show that there is an out-of-equilibrium pathway that can be used to escape a kinetically arrested state as well as a diverging time scale for phase separation as the critical frequency for condensation is approached. Rather than fine tuning the strength of the interactions among particles, a simple annealing scheme - toggling of the magnetic field - is used to create a broad envelope for assembly of ordered particle structures.

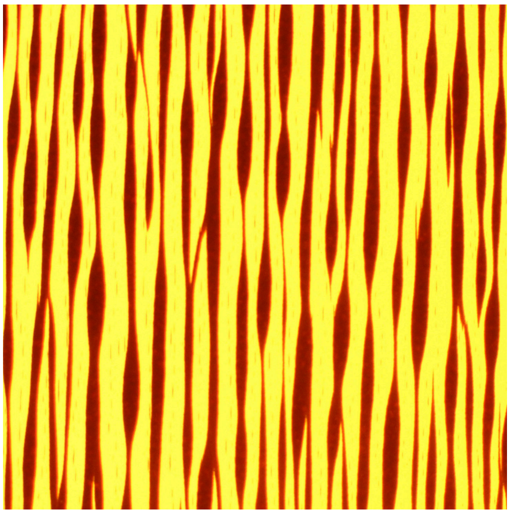

REFERENCES: [1] Swan, J. W.; Vasquez, P. A.; Whitson, P. A.; Fincke, E. M.; Wakata, K.; Magnus, S. H.; Winne, F. De; Barratt, M. R.; Agui, J. H.; Green, R. D.; et al. “Multi-scale kinetics of a field-directed colloidal phase transition,” *Proc. Natl. Acad. Sci. U. S. A.* **2012**, 109, 16023–16028. [2] Swan, J. W.; Bauer, J. L.; Liu, Y; Furst, E. M. “Directed colloidal self-assembly in toggled magnetic fields,” *Soft Matter* **2014**, 10, 1102–1109.

Invited Lecture

Nanofluidic Brownian Motors

Armin W. Knoll[1], M. J. Skaug[1], S. Fringes[1]
[1] IBM Research-Zurich, Säumerstrasse 4, CH-8803 Rüschlikon, Switzerland.

Inspired by the transport principle of molecular motors in cells, artificial Brownian motors have been studied theoretically and experimentally [1] to achieve directed motion and sorting of typically micron sized particles in fluidic environments. Ingredients of such Brownian motors are a spatially asymmetric potential landscape and unbiased external inputs driving the system out of equilibrium.

Here we describe a Brownian motor concept which effectively works for 60 nm gold spheres and should scale to even smaller particle dimensions. For this we exploit the interaction potential of the gold spheres to like charged confining surfaces in a nanofluidic slit. We shape a laterally asymmetric potential landscape by patterning a 3D ratchet topography in one of the two confining surfaces using thermal scanning probe lithography [2] and drive the system by applying a zero-mean AC electric field. We use interference scattering interferometry (iSCAT) [3] to track the particle motion with <10 nm spatial and <2 ms temporal resolution. Furthermore, our experimental setup allows us to tune the distance of the confining surfaces with nanometer precision. We study the time-resolved performance of the Brownian motors as function of applied voltage, frequency and gap distance. We observe a net particle drift of up to 100 microns per second along the direction dictated by the ratchet geometry. All relevant physical quantities can be measured *in-situ* enabling a parameter free comparison to theory. Our concept works on highly scaled ratchet tracks having a track width of <100 nm and a curvature down to 1 µm radius (Fig. 1). The performance depends strongly on gap separation which indicates a high selectivity to particle size. Thus we envision a highly selective sorting platform for any kind of sufficiently charged particles such as carbon nanotubes, DNA and proteins.

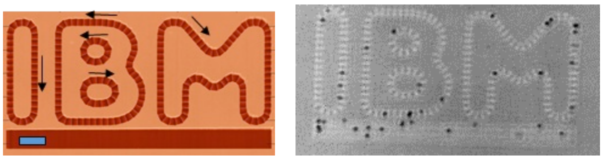

Figure 1: Left: AFM topography defining the Brownian motor energy landscape. Arrows indicate the motor direction. Scale bar is 2 um. Right: iSCAT optical snapshot of the working device.

REFERENCES: [1] Hänggi et al. *Rev. Mod. Phys.*, **2009**, *81*, 387 [2] D. Pires et al., *Science* **2010**, *328*, 732. [3] P. Kukura et al., *Nature Methods* **2009**, *6*, 923.

ACKNOWLEDGEMENTS: This work was funded by the ERC Starting Grant. no. 307079 (Topoplan).

Shear rheology of polystyrene melts and solutions with the same number of entanglements

Salvatore Costanzo[1,2], Giovanni Ianniruberto[3], Giuseppe Marrucci[3], Dimitris Vlassopoulos[1,2]

[1] Institute of Electronic Structure and Laser, FORTH, Heraklion 71110, Crete, Greece.

[2] Department of Material Science & Technology, University of Crete, Heraklion, 71003, Crete, Greece. [3] Dipartimento di Ingegneria Chimica, Università "Federico II", P.le Tecchio 80, 80125, Napoli, Italy.

INTRODUCTION: Polystyrene (PS) melts and solutions with the same number of entanglements (Z) exhibit identical reduced linear viscoelastic properties. Conversely, due to their lower friction reduction potential, solutions behave differently from melts in nonlinear extensional flow [1]. This difference is not observed in nonlinear shear flow. The main features of the transient shear response, i.e. viscosity overshoot, followed by undershoot at very high shear rates, and eventually steady state, are investigated systematically with careful measurements using cone-partioned plate fixture, and rationalized based on the concept of molecular tumbling of polymer chains, induced by the vorticity of the velocity gradient tensor in shear flow. A tube-based model including tumbling describes the experimental data well.

METHODS: We investigated the linear and nonlinear shear rheology of two PS melts having different molecular weights, namely PS133k (Z=10) and PS185k (Z=13.9), and two different PS solutions prepared by diluting PS285k with PS2k at two different concentrations, namely 47% (Z=10) and 65% (Z=13.9). Linear and Nonlinear measurements were performed on an ARES rheometer using a home-made cone-partitioned plate geometry to prevent artefacts induced by edge fracture instability [2].

RESULTS: The transient viscosity of melts and solutions, was recorded at different shear rates, $\dot{\gamma}$. The upper panel of Figure 1 depicts the normalized steady state transient viscosity as a function of the Weissenberg number based on the terminal time, τ_m ($Wi_m = \tau_m\dot{\gamma}$). Contrary to extensional data, all shear data collapse on the same master curve with a slope of -0.82, suggesting that friction reduction does not play a significant role in shear flow. We propose that the vorticity of the shear flow field causes molecules to tumble, hence preventing strong alignment in the flow direction. The lower panel of Figure 1 shows an example of the predictions of a tubemodel with tumbling. Very good agreement is observed between data and predictions. On the other hand, without the tumbling contribution the model fails in predicting the experimental data.

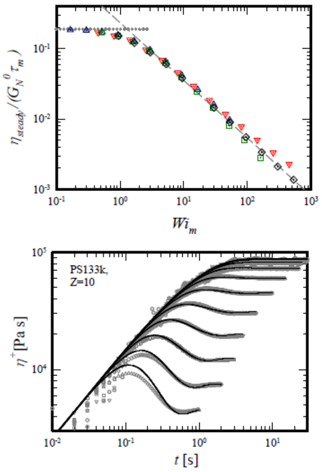

Fig 1: Universal scaling of PS melts and solutions in shear flow (upper panel, symbols: PS185k green, PS133k blue, PS285k-2k-65 black, PS285k-2k-47 red). Transient viscosity of PS 133k (lower panel, grey symbols: data, lines: predictions).

DISCUSSION & CONCLUSIONS: Our results demonstrate that the differences found in extensional flow between melts and solutions are not detectable in shear flows up to the maximum Weissenberg number reached, because of molecular tumbling. The predictions of the proposed model accounting for tumbling show good agreement with experimental data. In particular, this leads us to propose that, in the absence of wall slip, tumbling is at the origin of transient stress undershoot at high shear rates.

REFERENCES: [1] Huang et al., *Macromolecules*, **2015**, 48, 4158-4163. [2] Snijkers et al., *Journal of Rheology*, **2011**, 55, 1167-118.

ACKNOWLEDGEMENTS: EU Supolen project for support, Dr. F. Snijkers (CNRS-Solvey, Lyon) for discussions.

Viscoelastic spectrum of sheared model hard sphere and interpenetrable soft colloidal glasses

A. R. Jacob[1], A. S. Poulos[2], S. Kim[3], J. Vermant[4], G. Petekidis[1]

[1] *IESL-FORTH & Materials Science & Technology Department, University of Crete, Heraklion, Greece.* [2] *Jülich Centre for Neutron Science (JCNS-1) and Institute for Complex Systems (ICS-1),Forschungszentrum Jülich GmbH, Jülich, Germany.* [3] *Chemical Engineering Department, Katholieke Universiteit Leuven, Heverlee, Belgium.* [4] *Department of Materials, ETH Zürich, Zürich, Switzerland.*

INTRODUCTION: The flow of glasses is an intriguing subject in condensed matter physics, both of fundamental interest and technological importance, in a variety of systems from polymers and colloids [1] to spin and metallic glasses [2]. In this work model hard sphere and interpenetrable soft sphere colloidal suspensions in glassy states are investigated with orthogonal superposition rheomtery (OSR). We measure the full viscoelastic spectrum of sheared glasses through OSR and determine the characteristic crossover frequency ωc, which provides a direct measure of the shear induced structural relaxation. Transient start-up shear for both systems are also investigated with OSR.

METHODS: We used sterically stabilized poly(methyl methacrylate) (PMMA) nearly hard-sphere particles of 196 nm radius with polydispersity $\sigma \simeq 20\%$, dispersed in an octadecene-bromonaphthalene solvent mixture. Poly (ethylene-alt-propylene)-poly(ethylene oxide) (PEP-PEO) block copolymers form star like micelles in deuterium oxide (D_2O) with an aggregation number of 120. Superposition rheometry was performed using an ARES-G2 (TA) rheometer with a home modified normal force control loop, equipped with a custom built open bottom double wall Couette geometry [3]. Steady shear flow was imposed in the tangential direction and the small strain amplitude oscillatory motion was imposed vertically. We investigated steady state shear rates from 10^{-4} to 1 s^{-1}. Complementarily, we also conducted Brownian dynamics (BD) simulations using 50000 particles with 10% polydispersity for $\phi = 0.62$.

RESULTS: A Shear Rate Orthogonal Frequency Superposition (SROFS) is achieved for both systems but deviations are observed mainly for the hard sphere colloidal glasses in short and long time scales (see Fig. 1). Horizontal Scaling factor of SROFS, the colloidal analogoue to Time Temperature Superposition, provides insight into the timescales present under shear and the vertical scaling factor points to the in-cage free volume of the system. The crossover frequency extracted from the linear viscoelastic spectra varies linearly with shear rate for hard spheres, and sub-linearly for the soft interpenetrable star-like micelles. Brownian Dynamics simulations show that anisotropic cage structure is responsible for the deviations in hard sphere glasses in short time scales. The long time deviations in hard sphere glasses is speculated to be due to hydro-cluster formations.

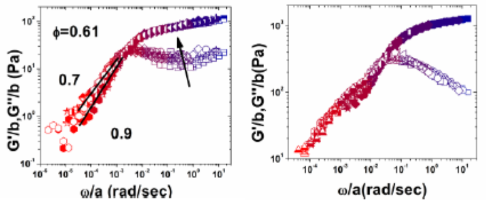

Fig. 1: SROFS for Hard Sphere glass at φ=0.61 (left) and Star like Micelles at c/c = 350 (right). The blue to red color indicates steady shear from low to high shear rates.*

DISCUSSION & CONCLUSIONS: We are able to measure for the first time the full viscoelastic spectra of sheared hard sphere [4] and soft colloidal glass and obtain a scaled map of the dynamics of the system through a strain rate-orthogonal frequency superposition.

REFERENCES: [1] J. Mewis and N. J. Wagner, Colloidal Suspension Rheology (*Cambridge Series in Chemical Engineering*, Cambridge, England, **2012**). [2] F. Spaepen; **1977**; *Acta Metall.*; 25:407. [3] J. Vermant *et. al.*; **1997**; *Rev. Sci. Instrum.*; 68:4090. [4] A. R. Jacob *et. al.*; **2015**; *Phys. Rev. Lett.*; 115:218301.

ACKNOWLEDGEMENTS: We thank Andy Schofield for particle synthesis and N. Koumakis, E. Moghimi, and A. Papagiannopoulos for discussions. We acknowledge funding from EU project "ESMI," Greek National funding through Grant THALES "Covisco" and ARISTEIA II "MicroSoft", and the Swiss National Science Foundation Grant No SNF 200021_157147. A. S. P acknowledges financial support from the DFG (Project No. SFB-TR6).

Soft apple cells suspensions: How does structural parameters and continuous phase impact rheological behaviour?

C. Leverrier, G. Almeida, G. Cuvelier

UMR Ingénérie Procédés Aliments, AgroParisTech, Inra, Université Paris-Saclay, Massy, France

INTRODUCTION: Rheological behaviour of soft particles suspensions is known to be influenced by the particle micromechanics and the phase volume. However, whether the insoluble solids content (*i.e.* plant cell walls) has been identified as a major parameter governing processed fruit and vegetable suspensions rheology, the phase volume of fruit and vegetable cells is not well defined yet [1].

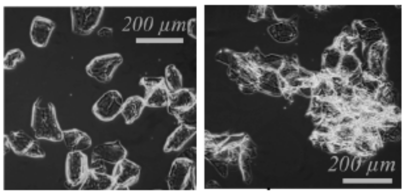

Fig. 1 – Optical microscopy of apple cells (left) and apple cell cluster (right)

Indeed, fruit and vegetable cells are soft particles whose size and volume can change under stress. They are able to highly deform and pack, with no specific form. Moreover, less than 1% of cells walls is sufficient to create a network between the particles leading to a weak-gel behaviour. The actual study focus on the impact of structural parameters (size, shape and polydispersity) and continuous phase on the rheological behaviour of apple cells suspensions.

Table 1 – Properties of the continuous phases used

	Distilled water	NaCl 0.1%	Sucrose 48%m	Apple serum	CMC 1%	CMC 3.2%
η *mPa.s*	1	1	13	13	13	108
ρ *g.cm^{-3}*	1.000	1.000	1.219	1.051	1.006	1.018
IS *µS/cm*	0.80	1750	18	1730	2000	6000

METHODS: Two model suspensions of monomodal apple particles (d50 of 220µm and of 440µm, Fig. 1) were prepared. Apple puree was ground, sorted by size and washed by wet-sieving prior to drying by solvent exchange in order to obtain size-controlled dried apple particles. These particles were dispersed in five controlled aqueous media varying in composition, viscosity, pH and ionic strength (*Table 1*). Up to twenty levels of particle content were prepared in each model medium. To validate the relevance of the model and to see the impact of polydispersity, apple particles were also dispersed in the original continuous phase of its (apple serum) and compared to original apple purees of several grinding levels.

RESULTS: Rheological parameters (apparent viscosity, yield stress, storage modulus) increase with the particle size and the particle content. **Three concentration domains** are observed, whatever the particle size or continuous phase, both in flow (*Fig.2A*) and in dynamic measurements. In the first domain, suspensions exhibit Newtonian flow. Particles size, shape and polydispersity have little effect on rheology. Ionic strength appears to impact only when the ionic strength of the continuous phase is close to zero (distilled water) which increases the viscosity probably due to electrostatic repulsions. Elastic properties appear in the intermediate domain (*Fig.2B*). Particles size and shape have an effect on rheology. Viscosity and ionic strength of the continuous phase impact the elastic modulus in this domain. In the third domain, the dependency between viscosity and concentration is less pronounced. The impact of continuous phase in this domain is greatly reduced.

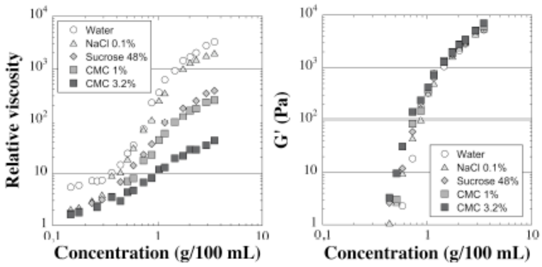

Fig. 2 – Relative viscosity and Elastic modulus as a function of insoluble solids content for 220µm particles

DISCUSSION & CONCLUSIONS: This study confirms that particle content and morphology have a major impact on rheological behaviour of apple cells dispersions. Three concentration regimes were highlighted:

- In the **diluted domain**, electrostatic repulsion between particles can be observed. But size and shape seem to have no significant effect.
- The **intermediate domain** is characterised by the building of a weak network between particles.
- In the **concentrated domain**, particles begin to pack. The crowding of particles and their interactions govern the elastic properties in this domain.

REFERENCES: [1] Day et al. **2010**; *Food and Bioprocess Technology* ; 3:928–934.

Aggregation kinetic of magneto-rheological fluids under confinement

Keshvad Shahrivar, Elizabeth Carreón-González and Juan de Vicente

Department of Applied Physics, Faculty of Sciences, University of Granada, C/Fuentenueva s/n, 18071 Granada, Spain

kshahrivar@ugr.es

INTRODUCTION: MR fluids are colloidal dispersions of micrometer-sized magnetizable particles in some carrier fluid which, due to interaction among these induced-dipoles undergo process of structure formation and particles aggregate into chainlike structure aligned with external field. The aggregation kinetics of magnetic colloidal suspensions has been the subject of great interest over the last decade mostly concerning magnetic micron-sized latexes[1]. In spite of importance of MR applications, the aggregation kinetics of carbonyl iron suspensions have not been studied thoroughly.

METHODS: In this work microstructure formation of carbonyl iron based magneto-rheological fluids under confinement was studied using Stokesian dynamics simulation and optical microscopy and image analysis method. Micro-channels of different cross sections were used ranging from 250 µm to 1000 µm in width and constant height of 100 µm. Homemade micro-rectangular tubing fabricated using lithographic technique was used to hold the MRF suspension (CIP grade EW) on microscope.

RESULTS: The simulation results show that mean clusters size, at low concentrations $\phi_{2D} \leq 0.05$, follow asymptotic power-law behavior in agreement with aggregation scaling theory. In an interesting way, all curves can be collapsed on a master curve using a characteristic time. In this particular case this characteristic time, obtained from simulation, has been found to be $t_{scaling} \propto \frac{1}{\lambda \phi_{2D}^{2.614} L^{0.23}}$. Figure 1 shows collapse of evolution of experimental mean cluster size as a function of scaled time ($\tilde{t} = \frac{t}{t_{scaling}}$) obtained from simulation. The experimental data shows a good agreement with simulation prediction at higher times although at short times experimental data have higher values.

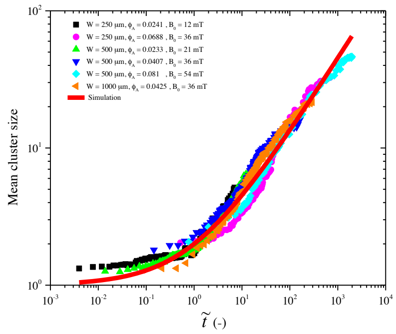

Figure1. Evolution of mean cluster size

REFERENCES: [1] M. Fermigier, A. P. Gast, and A. P. Gast, “Structure evolution in a paramagnetic latex suspension,” *J. Magn. Magn. Mater.*, vol. 122, no. 1–3, pp. 46–50, Dec. **1993**.

ACKNOWLEDGMENTS: This work was supported by MINECO MAT 2013-44429-R and PCIN-2015-051 projects (Spain), European Regional Development Fund (ERDF) and by Junta de Andalucía P10-RNM-6630 and P11-FQM-7074 projects (Spain). EC-G acknowledges the financial support by CONACYT (Ref #232347)

Dielectrophoretic Tweezers

Ahmet F. Demirörs[1], André R. Studart[1]
[1] *ETH Zürich, Complex Materials, Zürich, Switzerland.*

External field gradients are commonly used for separation, contactless manipulation and assembly of nano- and microparticles. Here, we introduce a novel tweezing technique by using electric field gradients, so called dielectrophoresis. In a homogenous electric field, a dielectric colloid can act as a field gradient-maker, by changing the electric field strength around itself. Such field strength alteration around the dielectric colloid can be employed as a trap for other particles. Orthogonally using magnetic fields in addition to electric fields and employing magnetic "Tweezer-colloids" enables loading, transporting and unloading of the trapped cargo.

RESULTS: Figure 1 demonstrates an example of how electric fields are used to trap and finally unload the particles, while using magnetic forces for transport of the cluster.

ACKNOWLEDGEMENTS: AFD and ARS are grateful for the financial support from the Swiss National Science Foundation (grants 200021_126646 and PZ00P2_148040).

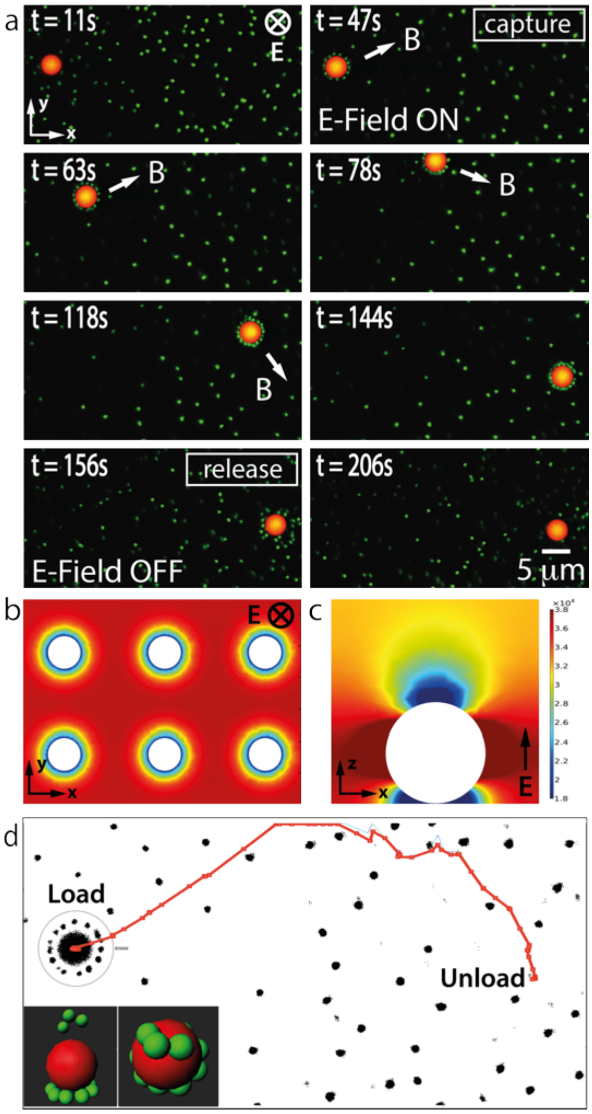

Fig. 1: (a) Trap, transfer and delivery of tweezes (cargo) by a superparamagnetic probe colloid. An external magnetic field [B] is used to transfer the particles whereas electric field is used to trap and release the tweezed colloids. Panels in time steps show the initially free particles are trapped around the larger superparamagnetic (red) particle by the application of an electric field. (b-c) Calculations of the electric field strength around such probe particles (red in (a)) in xy plane (b) and xz plane (c). (d) The path that the probe-colloid and its load followed throughout the images presented in (a).

Insights into the mechanisms of capillary assembly

S. Ni[1,2], J. Leemann[1,2], A. Omeradzic[3], M. Thielmann[3], H. J. Herrmann[3], H. Wolf[2] and L. Isa[1]

[1] Laboratory for Interfaces, Soft Matter and Assembly, Department of Materials, ETH Zurich, Vladimir-Prelog-Weg 5, 8093 Zurich, Switzerland. [2] IBM Research – Zurich, Säumerstrasse 4, CH-8803 Rüschlikon, Switzerland [3] Computational Physics for Engineering Materials, Institut f. Baustoffe (IfB), ETH Zürich, CH-8093 Zürich, Switzerland

Capillarity – assisted particle assembly trapped on topographically structured templates has been widely explored in micro- and nanofabrication, for nanoelectronics [1], bioanalysis [2] and plasmonics [3]. The advantages of capillary assembly include a broad range of applicable particle sizes, accurate placement with nanometric precision and little limitation on particle material. However, scarce knowledge has been gathered to date concerning the impact of the trap geometry, and in particular trap depth, on assembly results. Here we show that the assembly results vary as a function of the trap depth, when the length of the traps allows for more than one particle to be assembled. By increasing the depth of the traps, the results change from trapping one particle only to complete trap filling. Confocal microscopy is employed to extract the local motion of particles during trapping. A systematic investigation is carried out to map the results obtained with a series of trap depths and surface tensions. A qualitative model supported by numerical simulations is used to elucidate the underlying mechanism of the observed assembly results. Trapping of one particle is favoured with a shallow trap and a moderate surface tension. A subsequent refilling step enables assembly of another type of particle next to the assembled one (Figure 1). The new finding opens up a new strategy to fabricate anisotropic and heterogeneous particle clusters [4].

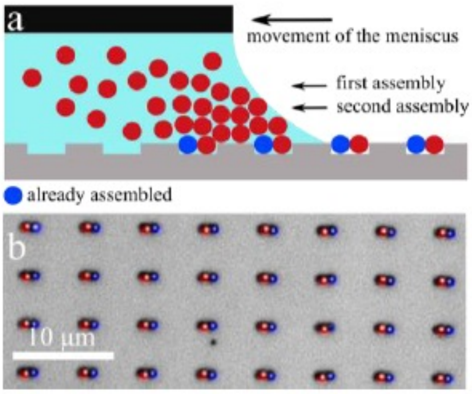

Fig. 1: Schematic illustration of sequential capillary assembly (a), stepwise filling of the trap with different particles (b) [4].

REFERENCES: [1] Y. Cui, M. T. Björk, J. A. Liddle, C. Sönnichsen, B. Boussert and A. P. Alivisatos, *Nano Lett.*, **2004**, 4, 1093–1098. [2] A. Cerf, H. C. Tian and H. G. Craighead, ACS Nano, **2012**, 6, 7928–7934. [3] J. A. Fan, K. Bao, L. Sun, J. Bao, V. N. Manoharan, P. Nordlander and F. Capasso, *Nano Lett.*, **2012**, 12, 5318–5324. [4] S. Ni, J. Leeman, H. Wolf and L. Isa, *Faraday Discussions*, **2015**, 181: 225-242.

ACKNOWLEDGEMENTS: The authors thank Ute Drechsler and Steffen Reidt for help on the mask and master fabrication, Joachim Hehl, Xander van Kooten, Tobias Kraus, Armin Knoll and Urs Duerig for useful discussions and advice, Rolf Allenspach and Walter Riess for continuous support. LI and SN acknowledge financial support from the Swiss National Science Foundation grant PP00P2_144646/1.

Charge spectrometry on single macromolecules in solution

F. Ruggeri[1] , F. Zosel[2] , B. Schuler[2] & M. Krishnan[1,3]

[1]*Department of Chemistry, Winterthurerstrasse 190, University of Zurich, CH 8057 Zurich, Switzerland,* [2]*Department of Biochemistry, Winterthurerstrasse 190, University of Zurich, CH 8057 Zurich, Switzerland,* [3]*Department of Physics, Winterthurerstrasse 190, University of Zurich, CH 8057 Zurich, Switzerland*

INTRODUCTION: Electrical charge is a fundamental property of biomolecules, strongly influencing their function [1] and stability. We demonstrate for the first time a high-precision (<1*e*), absolute measurement of the electrical charge of biomolecules in solution. The method is based on parallel, external field-free trapping [2] at an unprecedentedly low estimated sensitivity of yoctomoles (1-10 molecules). The ability to experimentally link macromolecular charge and structure will open up a new physical dimension in biology.

METHODS: Our single molecule trap is created in a fluid-filled gap between two charged walls. Nanoscale patterning of one of the surfaces leads to a modulation of the local electrostatic potential, creating a deep thermodynamic potential well for a like-charged entity. In our new method "Escape Time Electrometry" (ET*e*) we measure the time that a charged molecule in solution takes to leave the potential well, whose depth (F) is linearly proportional to the effective charge (q_m) of the molecule (Fig. 1 a-b). A molecule undergoing Brownian motion will resides in a trap for a time (t_{esc}) given by Kramer's analytical expression,

$$t_{esc} = t_r exp(F/k_B T) \qquad (1)$$

where t_r is the relaxation time of the molecule. When occupied by a fluorescently-labelled molecule the optical intensity of the trap region is high (Fig. 1c). The duration of the intensity bursts (Δt) follows an exponentially decaying probability distribution $P_n(\Delta t)$, which is fitted to extract t_{esc} .

RESULTS: ET*e* allows a direct measurement of the effective charge (q_m) of molecules, which can be theoretically modelled and related to the molecule's known structural charge (q_{str}); Table 1 summarizes a few representative results. The measured charge of DNA molecules is in remarkable agreement with existing theoretical predictions [3] and suggest that ET*e* can serve to readout the inter-nucleotides spacing of an arbitrary nucleic acid molecule or polyelectrolyte. The study of the enzyme Gusβ suggests substantial regulation of the structural charge in a globular molecule [4], while our measurements on Protα, a disordered onedimensional polypeptide, provides unique insight into the charge renormalizing behaviour of short, strongly charged segments within the molecule. Furthermore the exponential dependence of t_{esc} on the charge of the molecule permits us to distinguish between two Protα variants that differ by a mutation of a single amino acid (E59K, 4% of the structural charge) (Fig. 1d).

Table 1. Comparison of the structural (q_{str}) and measured charge (q_m) of some of the molecules studied.

Molecule	q_{str}	q_m
ssDNA, 10b	13	11.5±0.5
ssDNA, 20b	23	15.6±0.6
dsDNA, 60bp	124	38±1.2
Protα	46	34.9±0.6
ProtαE59K	44	32.1±1.6
Gusβ	133.8	31.4±1.1

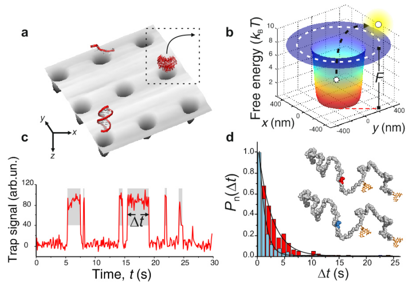

Fig. 1: ETe: Schematic of trapped biomolecules. (a) AFM image of a trap array. (b) Calculated 2d potential distribution in a trap. (c)Temporal intensity trace of the optical signal from a trap. (d)Escape time normalized probability distribution $P_n(\Delta t)$. Two variants of Protα with a single amino acid mutated from negatively charged (red) to positively (blue). The difference in charge of 2e gives the former a factor 2 longer t_{esc}.

DISCUSSION & CONCLUSIONS: The ability to sensitively detect small changes in net charge and the dependence of this measurable on 3D molecular conformation could have wide- ranging implications in structural biology, making ET*e* a new tool for ultrasensitive, rapid structural studies on biological macromolecules in the fluid phase.

REFERENCES: [1] Perutz, **1978**; *Science*; 201:1187- 1191. [2] Krishnan et al.; **2010**; *Nature* 467:692-695. [3] Manning, **1969***; Journal of Chemical Physics*; 51:924-& 492. [4] Ninham, Parsegian, **1971***;Journal of Theoretical Biology*; 31:405-428

Contact line around spherical particles trapped at anisotropic fluid interfaces.

N. Senbil[1,2], A.D. Dinsmore[2]

[1] University of Fribourg, Fribourg, Switzerland. [2] University of Massachusetts, Amherst, MA, USA

INTRODUCTION: A spherical particle trapped at a fluid interface forms a contact line where the solid and the two immiscible fluids meet. The shape of the contact line is the key to determining the overall interface shape and capillary interactions with other particles. At a planar interface, the contact line is a circle. When the interface has anisotropic curvature, however, the leading order deformation of the contact line has quadrupolar (cos(2*phi)) symmetry [1]. In our experiments, we measure the quadrupolar deformation at different anisotopic fluid interfaces and compare with the theory [2].

METHODS: PDMS-coated glass spheres with diameter 2.4 and 3.2 mm are used. We verify that there is no observable pinning on the surface and repeatable results could be measured [3].

To make fluid interfaces with anisotropic shape, two razor blades are placed in a way that sharp edges face each other. The container is filled with water. The fluid interface is pinned at the tips of the razor blades and the air-water interface adopts a semi-cylindrical shape. By adding or removing water, the curvature anisotropy of the fluid interface is adjusted. The deviatoric curvature, D_0, is defined as half the difference between the two principal curvatures of the interface.

RESULTS: In our experiments D_0 ranges from 0 to 0.21 mm$_{-1}$. Our experience shows that the steady state conditions for advancing and receding are different. Thus, we measure quadrupolar deformation, z_2, for advancing and receding states separately ($z_{2,A}$ and $z_{2,R}$). The relation between D_0 and z_2 is given as:

$$z_2 = D_0 r_{c2}/6 \qquad (1)$$

where r_c is the radius of the contact line around the sphere. However, the prediction [2] is valid for $aD_0 << 0$ and for zero capillary force. However, in our measurements there is a capillary force, which balances a vertical pushing force applied to the sphere. Thus, we extrapolate the values of z_2 where capillary force is zero. Two independent methods are used and compared to theory. Both methods agree well with the theory at small D_0 as seen in Fig. 1.At a given D_0, z_2 depends highly on r_c; for instance when the contact line is near the equator, z_2 is much bigger than when it is near the poles.

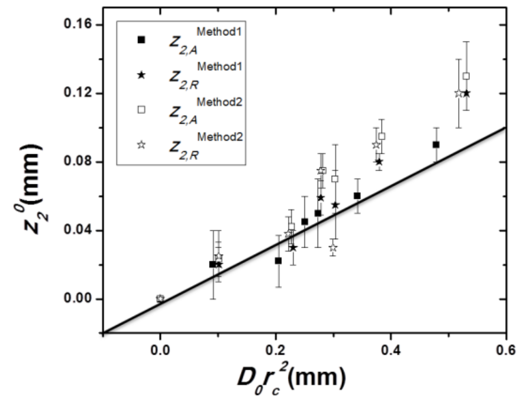

Fig. 1: Comparison of both methods 1,2 for advancing and receding cases (A,R) with the theory (solid line).

DISCUSSION & CONCLUSIONS: Our results are the first, to our knowledge, where the shapes of the contact line around a sphere at a curved interface is directly measured and numerical results are given. We show that z_2 depends on D_0, r_c, F_{cap} and agrees with the existing prediction for advancing contacts but not for receding. Since the contact angle used in the prediction is Young-Dupre angle, this might mean that advancing contact angle is closer to equilibrium compared to the receding angle. Our results are important to understand colloid interactions at fluid interfaces.

REFERENCES: [1] Wurger A (**2006**) Curvature-induced capillary interaction of spherical particles at a liquid interface. *Physical review. E, Statistical, nonlinear, and soft matter physics* 74(4 Pt 1):041402. [2] Zeng C, Brau F, Davidovitch B, & Dinsmore AD (**2012**) Capillary interactions among spherical particles at curved liquid interfaces. *Soft Matter* 8:8582--8594. [3] Senbil N, He W, Demery V, & Dinsmore AD (**2015**) Effect of interface shape on advancing and receding fluid-contact angles around spherical particles. *Soft Matter* 11(25):4999-5003.

ACKNOWLEDGEMENTS: This research was made possible in part by a grant from BP/The Gulf of Mexico Research Initiative through the C-MEDS consortium, and in part by the U.S. National Science Foundation (CBET-0967620).

Biomimetic engineering of polymersome membranes for stimuli triggered activity of nanoreactors

T. Einfalt[1], R. Goers[1,2], I.A Dinu[1], A. Najer[1], M. Spulber[1], O. Onaca-Fischer[1], C.G. Palivan[1]

[1] University of Basel, Basel, Switzerland. [2] ETH Zürich, Zürich, Switzerland.

INTRODUCTION: The development of advanced stimuli-responsive systems for medicine, catalysis or technology requires compartmentalized reaction spaces with triggered functionality. An elegant nano-science-based strategy is to engineer such compartments with triggered activity by encapsulation/insertion of active compounds in compartments with stimuli-responsive permeability. Here, we introduce nanoreactors with pH-triggered activity based on polymersomes with encapsulated enzymes and a membrane equipped with modified channel proteins, acting as "gates" (Fig. 1). By insertion of a chemically modified porin with a pH-sensitive molecular cap we obtained a selective permeability of the membrane. The substrate can penetrate inside the cavity and the enzymatic reaction takes place only when the gate is open (by releasing its pH-sensitive cap) [1]. Then the products are released from the nanoreactor.

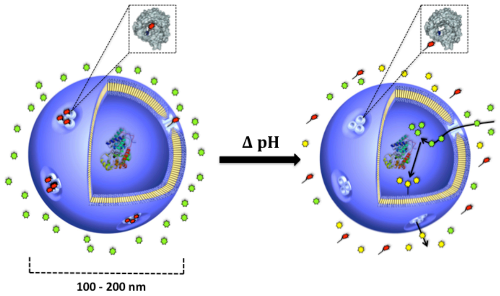

Fig. 1. Concept of a nanoreactor with triggered activity by a chemically engineered protein "gate" inserted in a polymersome membrane. A change in pH induces the release of the sensitive molecular cap (green dots) from the protein "gate" allowing the entrance of substrates (red dots), and the release of the products of the enzymatic reaction (yellow dots).

METHODS: OmpF Modification. First, lysine residues were coupled with levulinic acid by a simple sulfo-NHS/EDC reaction, and unreacted levulinic acid was removed by filtration and dialysis. This step introduced reactive carbonyl groups to favor the binding of a pH responsive cap Cyanine5-hydrazide (Cy5-Hydrazide). Cy5-hydrazide was selected as the second part of the pH responsive linker, because its molecular weight (569.6 g/mol) matches with the pore size at the constriction region. pH-responsive nanoreactors were prepared from $PMOXA_6$-$PDMS_{44}$-$PMOXA_6$ copolymer, and a subset of modified or native OmpFs and horseradish peroxidase in PBS buffer pH=7.4. We used the film rehydration technique as being suited for enzymes and channel porins (films were rehydrated to a final polymer concentration of 5 mg/ml). All samples were extruded through a polycarbonate membrane in order to obtain size homogeneity. Non-encapsulated enzyme was removed from the nanoreactors by dialysis against PBS.

RESULTS: To assess how the nanoreactor activity was affected by the chemical modification of the porin, we used the Amplex Red enzymatic substrate. The enzymatic turnover of the Amplex Red substrate (predicted polar surface area 72 A2, MW = 257 g mol-1, Log P = 0.89, charge = -0.1 at pH 7.4) was drastically reduced (down to 14%), compared to OmpF-WT nanoreactors acting in similar conditions at pH = 7.4. The blockage of Amplex Red influx through the pore is considered to be due to a combination of effects: (i) closing of the pore by the molecular cap, and (ii) electrostatic interaction of Amplex Red with the molecular cap (Fig 2).

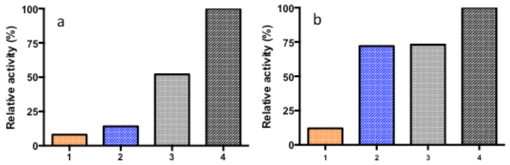

Fig.2: Amplex red conversion kinetics of nanoreactors equipped with different OmpFs: (1) unpermeabilised nanoreactors (orange), (2) OmpF-CA-Cy5 (blue), (3) OmpF-CA (grey), and (4) Ompf-WT (black) at pH 5.5, at time 0 (a) and after 1 hour (b).

CONCLUSION: We designed a nanoreactor with a pH responsive enzymatic activity, based on a che¬mically modified channel porin OmpF, which was inserted in the membrane of polymersomes, and acted as a "pH responsive gate". Our system has high potential for biosensing and therapeutical applications that will be further investigated.

REFERENCES: [1] Einfalt T.; Goers R.; Dinu I. A; Najer A.; Spubler M.; Onaca-Fischer O; Palivan C. G.. *Nano Lett*, **2015**, 15, 7596

Aligned crystallites in gyroid-forming triblock copolymer films

I. Gunkel[1], R. Dehmel[2], J. A. Dolan[2], B. D. Wilts[1], A. Sepe[1], Y. Gu[3], U. Wiesner[3], U. Steiner[1]

[1] Adolphe Merkle Institute, Fribourg, Switzerland. [2] University of Cambridge, Cambridge, UK.
[3] Cornell University, Ithaca, NY, USA.

INTRODUCTION: Semicrystalline-amorphous block copolymers (BCPs) represent an interesting class of polymeric materials. The morphology of these BCPs is governed by two competing self-organizing mechanisms: microphase separation (MPS) and crystallization. MPS favors the formation of nm length scale morphologies like spheres, gyroid, cylinders, or lamellae. Crystallization on the other hand favors the formation of alternating amorphous and crystalline layers [1]. If the amorphous (non-crystallizable) block is glassy, crystallization is forced to occur within the morphology created by MPS, which is referred to as *confined crystallization*. While confined crystallization has already been studied for simple morphologies like spheres, cylinders or lamellae, surprisingly little is known about crystallization in more complex bicontinuous structures [2]. Here, we investigated crystallization within a continuous cubic gyroid structure in films of rubbery-glassy-semicrystalline triblock copolymers.

METHODS: Gyroid-forming poly(isoprene)-*b*-poly(styrene)-*b*-poly(ethylene oxide) (ISO) triblock copolymers were synthesized by anionic polymerization as described elsewhere [3]. ISO films were prepared by spin coating from anisole solutions onto fluorine-doped tin oxide coated glass, or silicon substrates, followed by solvent annealing in chloroform vapor. Birefringence was observed by means of polarized optical microscopy (POM). Structural characterization was carried out using scanning electron microscopy (SEM), grazing-incidence small-angle and wide-angle X-ray scattering (GISAXS and GIWAXS).

RESULTS: ISO films assembled into a continuous gyroid network after solvent annealing as determined from SEM and GISAXS analysis. The presence of semicrystalline poly(ethylene oxide) (PEO) blocks in these films was confirmed by GIWAXS experiments. Two distinct birefringence patterns were observed in solvent annealed ISO films: spherulitic Maltese cross patterns and extended regions of uniform birefringence (Fig. 1). While spherulites are commonly observed in semicrystalline polymers and BCPs, domains of uniform birefringence were only reported for non-polymeric, fully crystalline materials so far. The birefringence in ISO films was found to disappear above the melting point of the semicrystalline PEO blocks as confirmed by *in situ* POM during heating. This implies the birefringence results from the crystalline layers in the PEO blocks.

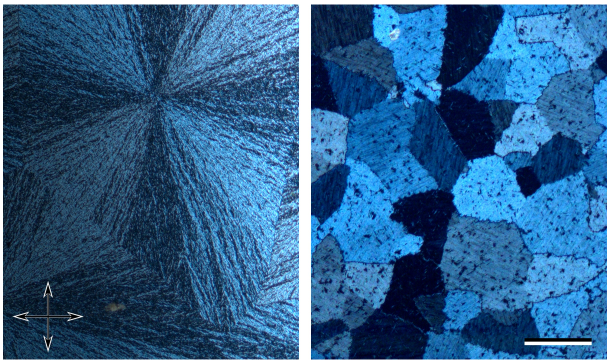

Fig. 1: Polarized optical micrographs of birefringent structures in thin ISO triblock copolymer films after solvent vapor annealing. Spherulitic Maltese crosses (left), and patterns of uniform domains (right). The scale bar is 200 µm.

DISCUSSION & CONCLUSIONS: Uniform birefringence in crystalline domains over nearly macroscopic distances (Fig. 1) implies large numbers of preferentially aligned crystallites. Interestingly, these domains were found to be congruent with gyroid domains of different orientation. This indicates a strong correlation between the preferentially aligned crystallites and the microphase-separated morphology, which has not been reported before.

REFERENCES: [1] Y.-L. Loo, R. A. Register, A. J. Ryan, **2002**; *Macromolecules*; 35:2365-2374. [2] W.-N. He, J.-T. Xu; **2012**; *Progress in Polymer Science*; 37:1350–1400. [3] J. G. Werner, T. N. Hoheisel, and U. Wiesner; **2014**; *ACS Nano;* 8:731–743.

ACKNOWLEDGEMENTS: We thank the Adolphe Merkle foundation for financial support. We acknowledge the assistance of D.M. Smilgies (CHESS, Cornell University) and C. Zhu (ALS, Berkeley Lab) with GISAXS and GIWAXS measurements.

Development of membrane mechanosensor

Roberto.D.Ortuso[1], Kaori Sugihara[1]

[1] *University of Geneva, Physical Chemistry Dept., 30 Quai Ernest Ansermet, 1205 Geneva, Switzerland.*

Membrane forces play pivotal roles in numerous physiological processes such as endocytosis, cell mutations and calcium signaling.

Currently used characterization methods such as atomic force microscope (AFM) or optical tweezers allow for the controlled force application but not for the detection of the forces applied to the bilayers. Micro-aspiration of giant unilamellar vesicles (GUV) enables the quantification of surface tension, however, its conversion into local forces is difficult.

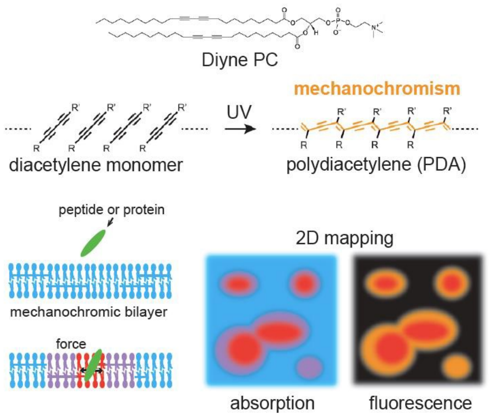

Figure 1: The chemical structure of DiynePC and polydiacetylene. The scheme shows the concept of the membrane force sensor we are developing.

We are developing a mechanosensitive membrane probe that enables direct measurement of molecular forces applied within lipid bilayers. We employ a mechanochromic polymer polydiacetylene (PDA, Figure 1) that changes its color and fluorescence intensity upon application of forces (Figure 2A-C). As a first step, we demonstrated a PDA vesicle assay that detects melittin, a transmembrane peptide from bee venom. First we fabricated PDA vesicles by self-assembling the lipid monomer and subsequently crosslinking by UV. Figure 2B shows the absorption spectra before (blue) and right after (red) addition of melittin to the PDA vesicle solution. These spectra overlap, suggesting no colorimetric response due to the addition of melittin. However, we found that the spectra shifted over the next several hours (Figure 2B). After 4 hours, the shape of the spectra changed completely, as the color change was clearly visible also by naked eyes (Figure 2C). The slow response from our PDA sensor against melittin is different from what has been reported with other types of PDA sensors [1, 2].

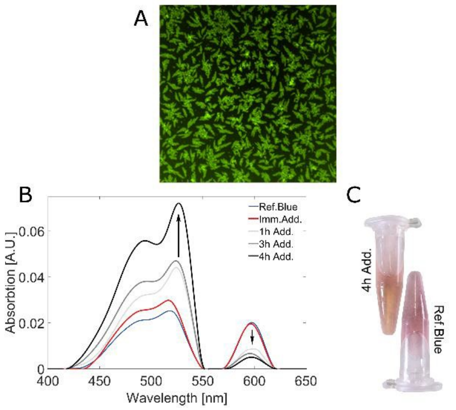

Figure 2: A. A fluorescent microscopy image of bilayers in 'Blue' state. B. UV-Vis spectra before and after the addition of melittin. A spectra shift was observed depending on the incubation time. C. An image of PDA vesicle samples before (below)

In this work, we further analyze the unexpectedly slow interaction kinetics, fluorescence spectra of PDAs, and discuss possible origin of the slow kinetics [3].

The developed assay proved that DiynePC PDA is sensitive to mechanical stimuli. The advantage of our PDA sensor is that it has a phosphocholine head group that mimics cell membranes. Its combination of sensitivity and the biocompatibility will allow us to incorporate this probe in live cells in future, providing us a further possibility to investigate force distribution during mitosis, cell migration, and interactions with medical implants etc.

REFERENCES: [1] Kolusheva, S., T. Shahal, and R. Jelinek. *Biochemistry*, **2000**. 39(51): p. 15851-15859. [2] Schrader, T. and E.V. *Topics in current chemistry*. **2007**, Berlin: Springer. Online-Ressource. [3] Robert D. Ortuso et al., *manuscript in preparation*.

ACKNOWLEDGEMENTS: Part of the research leading to these results has received funding from Swiss National Foundation (200021_162425).

Cis-to-Trans isomerization of C-C-double bond by single molecule force spectroscopy

Milad Radiom[1], Phally Kong[2], Plinio Maroni[1], Andreas F.M. Kilbinger[2], Michal Borkovec[1]

[1] University of Geneva and [2] University of Fribourg, Switzerland.

INTRODUCTION: Mechanophores are polymers whose structure contains force-responsive subunits. To actuate chemical reactions in mechanophores, mechanical force can be utilized instead of the conventional thermal, electrical, and photonic triggers [1]. Mechanical manipulation of mechanophores using atomic force microscopy (AFM) led to remarkable insights into the strength of various bonds. However isomerization mechanochemistry of double-bonds has not been investigated at the molecular level. We present our results of the force-induced *cis*-to-*trans* isomerization of C-C-double bond using AFM.

METHODS: Three C-C-double bond containing polymers were used. Structurally similar polymers that contained C-C-single bonds were used as control (*Fig. 1*). Single chains of polymers were stretched using AFM.

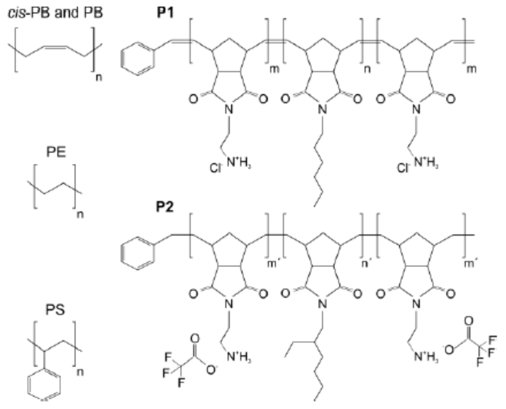

*Fig. 1: Structural formulas of the polymers used in this study: synthesized polymers **P1** and **P2**, cis-1,4- polybutadiene (cis-PB, cis 98%, trans 1%, vinyl 1%), 1,4-polybutadiene (PB, cis 36%, trans 55%, vinyl 9%), polyethylene (PE) and polystyrene (PS).*

RESULTS: Upon stretching C-C-double bond containing polymers (**P1**, *cis*-PB and PB) to elevated forces, a sudden relaxation in force and increase in elongation was observed in the force-extension profile (*Fig.* 2). Our results revealed an isomerization force of 800±220 pN (± is the standard deviation) (*Fig.* 3). Investigation of structurally similar polymers that did not contain C-C-double bond (**P2**, PE and PS) showed no trace of this transition.

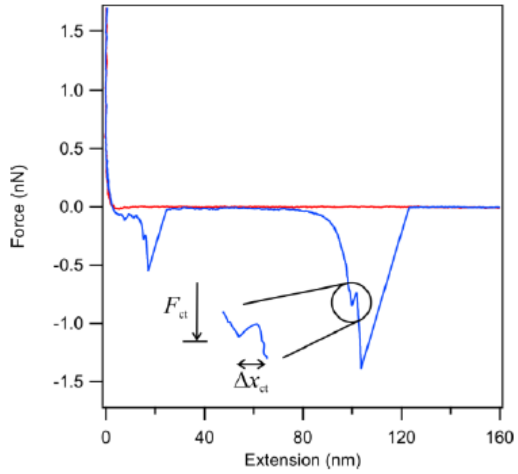

*Fig. 2: Force versus extension of **P1** showing an isomerization event. The onset of isomerization is denoted by force F_{ct} and elongation change Δx_{ct}.*

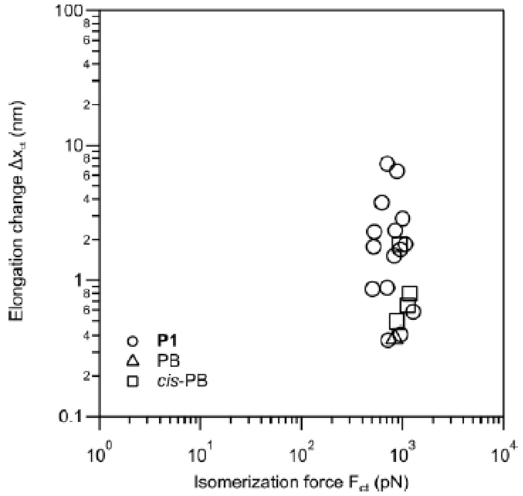

*Fig. 3: The elongation change Δx_{ct} of **P1**, PB, and cis-PB as a function of the isomerization force F_{ct}.*

DISCUSSION & CONCLUSION: Similar to ring-opening and covalent mechanochemistry [2, 3] isomerization mechanochemistry of C-C double bond revealed forces in range ~ 1nN (*Fig.* 3). Our results open the possibility of a new class of mechanophores based on C-C-double bond isomerization.

REFERENCES: [1] M.K. Beyer; *et al.*; *Chemical Reviews*; **2005**. [2] J. Wang; *et al.*; *Nature Chemistry* **2015**. [3] M. Grandbois; *at al.*; *Science*; **1999**.

ACKNOWLEDGEMENTS: Bio-Inspired Materials, NCCR, Switzerland. University of Geneva. University of Fribourg.

Posters

Microfluidic Diffusion Analysis of the Sizes, Interactions and Viscosities of Proteins under Native Solution Conditions

P. Arosio[1,^], T. Mueller[1,2], L. Rajah[1], E.V. Yates[1], F.A. Aprile[1], Y. Zhang[1], S.I.A. Cohen[1], D.A. White[1], T.W. Herling[1], E.J. De Genst[1], S Linse[3], M. Vendruscolo[1], C.M. Dobson[1], T.P.J. Knowles[1]
[1] Department of Chemistry, University of Cambridge, U.K., [2] Fluidic Analytics Ltd., Cambridge CB2 1EW, U.K., [3] Department of Biochemistry and Structural Biology, Lund University, SE
^current address: Department of Chemistry and Applied Biosciences, ETH Zurich, CH.

INTRODUCTION: Characterizing the sizes and interactions of macromolecules under native conditions is a challenging problem in many areas of molecular sciences, which fundamentally arises from the polydisperse nature of biomolecular mixtures. Moreover, interactions between macromolecules often lead to self-assembly and to an increase in the viscosity of the solution, which is a physical property of central relevance for a large number of applications in material, biological and biotechnological sciences.

METHODS: In this work, we propose an approach to measure the diffusion coefficients of specific species directly in solution by tracking simultaneously the spatial and the temporal evolution of their diffusion. We show that the acquisition of the diffusion profiles in two dimensions-space and time-increases the information content with respect to single profiles acquired in either space or time, and that such two-dimensional diffusion profiles can be modeled by diffusive and advection mass transport equations, resulting in the determination of accurate diffusion coefficients by rigorous interpretation of the experimental data without the need for any a priori knowledge of the analyte composition. We have implemented the concept of a single-step two-dimensional approach on a microfluidic platform, which offers a series of advantages over conventional techniques, including significant reductions in the amounts of sample and time that are required for the analysis as well as in the degree to which analytes interact with surfaces.

RESULTS: We show that the global analysis of such combined space−time data enables the hydrodynamic radii of individual species within mixtures to be determined directly by deconvoluting average signals into the contributions from the individual species. We demonstrate that the ability to perform rapid non-invasive sizing allows this method to be used to characterize interactions between biomolecules under native conditions. We illustrate the potential of the technique by implementing a single-step quantitative immunoassay that operates on a time scale of seconds and detects specific interactions between biomolecules within complex mixtures. Moreover, we demonstrate the use of the novel microfluidic technology to measure the viscosity of solutions by following the advection and diffusion of tracer particles. We validate our method with standard water-glycerol mixtures, and then we apply this microfluidic diffusion viscometer to measure the viscosity of protein solutions at high concentrations as well as of a crude cell lysate.

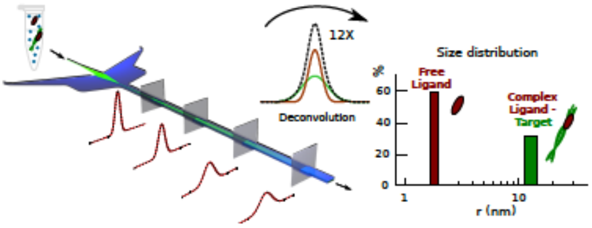

Fig. 1: Microfluidic space−time diffusion device for the analysis of size and interactions of proteins under native conditions.

DISCUSSION & CONCLUSIONS: In summary, we have demonstrated a microfluidic diffusion technique that is able to monitor quantitatively the diffusion of specific molecules in both space and time. The basis of this technique is the multidimensional acquisition of diffusion profiles at different diffusion times, which represents a fundamentally new development that allows high sizing resolution to be achieved by generating multiple contraints in the fitting of simulated diffusion profiles to experimental data. This approach allows the estimation of diffusion coefficients with high accuracy, thus enabling the definition of the average sizes and polydispersity of homogeneous and heterogeneous solutions.

REFERENCES: [1]P. Arosio et al., ACS Nano, 10, 333-341 (2016); [2]P. Arosio, et al., Anal. Chem., DOI: 10.1021/acs.analchem.5b02930 (2016)

Colloidal monolayers under steady and oscillatory shear at the liquid-liquid interface

Ivo Buttinoni[1], Zachary A. Zell[2], Mathias Steinacher[1], Todd M. Squires[2], Lucio Isa[1]
[1] *Department of Materials, ETH Zürich, Zürich, Switzerland* [2] *Department of Chemical Engineering, UCSB, Santa Barbara, USA*

INTRODUCTION: The macroscopic response of colloidal systems to shear and deformation is directly coupled to their microscopic structural evolution. Unfortunately, in most cases the use of macroscopic rheometers does not allow *in-situ* access to the system's microstructure at the single-particle level.

In this work we investigate the steady and oscillatory shear response of dense monolayers of charged colloids spread at a water/oil interface. In addition to 2D confinement, the presence of a liquid-liquid interface triggers the formation of crystalline regions with large lattice constants [1]. Following a novel active microrheological approach [2], a micro-fabricated magnetic disk is placed at the interface and rotated in a controlled fashion by external magnetic fields. Simultaneously, the structure of the sheared interface is imaged by optical microscopy and individual colloids are tracked.

RESULTS & DISCUSSION: Our observations emphasise the coupling between flow and structure in the sheared monolayer [3]. We measured the velocity profiles of the sheared suspension at different area fractions, shear rates, particle sizes and binary mixture compositions. At small shear rates, the monolayers flows via discreet hopping of the particles, i.e., the shear induced motion is defect-mediated. At larger applied rates, the flow induces ordering of the colloidal suspension around the disk, in the form of concentric rings. In the presence of binary mixtures, we report the alternation of layers of smaller and bigger particles. Increasing the shear rates even further, the bulk phases are also set significantly in motion and impose the flow field measured at the interface.

We also characterise, at the single-particle level, the viscoelastic response of interfacial colloidal monolayers to applied oscillatory shear flows. The mechanical properties of the 2D-colloidal crystal strongly depend on the amplitude and frequency of the applied perturbation: large amplitudes and small frequencies lead to irreversible plastic rearrangements that alter the monolayer crystalline microstructure.

REFERENCES: [1] T. S. Horozov, R. Aveyard, J.H. Clint, and B.P. Binks. *Langmuir*, 19(7), 2822-2829 (**2003**). [2] S.Q. Choi, S. Steltenkamp, J.A. Zasadzinski, and T.M. Squires. *Nature communications*, 2, 312 (**2011**). [3] I. Buttinoni, Z. A. Zell, T. M. Squires and L. Isa. *Soft Matter* 11(42), 8313-8321 (**2015**).

PEG brushes and their interaction with carbon dioxide

Anja Car[1], Gesine Gunkel-Grabole[1], Laurent Marot[2], Vikrant V. Naik[3], Gregor Ferk[4], Cornelia G. Palivan[1], Wolfgang P. Meier[1]

[1] University of Basel, Department of Chemistry, Klingelbergstrasse 80, CH-4056 Basel, [2] University of Basel, Department of Physics, Klingelbergstrasse 82, CH-4056 Basel, [3] ETH Zürich, Professur für Oberflächentechnik, Vladimir-Prelog Weg 1-5/10, CH-8093 Zürich, [4] Faculty of Chemistry and Chemical Engineering, Smetanova 17, 2000 Maribor

INTRODUCTION: Polymer brushes are polymer chains covalently attached to a solid substrate, and they provide a straightforward way to permanently modify the interfacial properties of surfaces. Thanks to the covalent connection between the polymer brush chain and an underlying substrate and the large variety of monomers available, they are successfully used in a plethora of areas where controlled surface properties are critical. Typical applications range from biocompatible surfaces to enhanced lubrication and energy storage.[1, 2] Moreover, polymer brushes are also applied to generate biomimetic membranes, particularly to prevent biofouling.[3, 4] Besides, porous substrates have been functionalized with polymer films for filtration applications of liquids, *e.g.* to purify fluids containing peptides or proteins,[5] but the concept of using them for gases is hardly explored. Polymers based on polyethylene glycol are frequently used to enhance the separation performance of the membranes, because the ethylene oxide groups specifically interact with carbon dioxide. [6] This effect was exploited in the polymeric multilayer gas separation membranes presented here. [7]

DISCUSSION & CONCLUSIONS: Thin poly(dimethylsiloxane) (PDMS) films were coated onto porous poly(acrylonitrile) (PAN) support material and subsequently functionalized with polymer brushes. Poly(oligoethylene glycol methyl ether)methacrylate (POEGMA) brushes were prepared by surface-initiated polymerization directly on a thin film of PDMS to yield a robust and flexible gas separation membrane. The polymerization of brushes directly from a PDMS film was facilitated by embedding a crosslinkable (atom transfer radical polymerization) ATRP initiator prior to curing of the film. It was confirmed by x-ray photoelectron spectroscopy that bromine groups used for initiation of ATRP are indeed available on the surface of the PDMS layer. Successful synthesis of the POEGMA brushes was shown by significantly altered surface properties shown in Fig.1.

The results presented here highlight the suitability of polymer brushes to modify the characteristics of gas separation devices. The flexibility and tunabiliy of surface properties offered by polymer brushes warrants their further exploration to widen the applications of separation membranes. and should be tab centered, with the number in parentheses on the right.

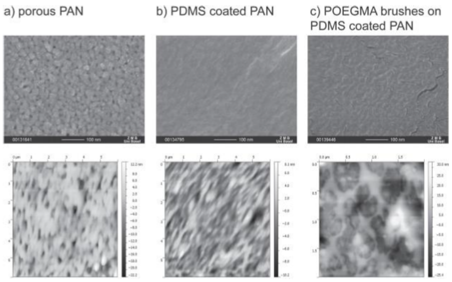

Fig. 1: Scanning electron microscopy and atomic force microscopy images showing surface morphology of the a) unmodified porous polyacrylonitrile membranes, b) the PAN after coating and curing a PDMS film containing ATRP initiator groups, and c) after polymerization of POEGMA brushes on top of the PDMS coating. SEM scale bars are 100 nm

REFERENCES: [1] O. Azzaroni, *J. Polym. Sci. A Polym. Chem.* **2012**, 50, 3225. [2] M. Chen, W. H. Briscoe, S. P. Armes, J. Klein, *Science* **2009**, 323, 1698. [3] J. Kowal, X. Zhang, I. A. Dinu, C. G. Palivan, W. Meier, *ACS Macro Lett.* **2014**, *3*, 59. [4] Y.-X. Shen, P. O. Saboe, I. T. Sines, M. Erbakan, M. Kumar, *J. Mem. Sci.* **2014**, *454*, 359. [5] J. Kowal, X. Zhang, I. A. Dinu, C. G. Palivan, W. Meier, *ACS Macro Lett.* **2014**, *3*, 59. [6] W. Yave, A. Car, K.-V. Peinemann, *J. Mem. Sci.* **2010**, *350*, 124. [7] G. Gunkel-Grabole, A. Car, V. V. Naik, L. Marot, G. Ferk, C. Palivan, W. Meier, *Macromol. Chem. Phys.* **2016** DOI: 10.1002/macp.201500450

ACKNOWLEDGEMENTS: This publication was supported by the Swiss National Science Foundation as part of the NCCR Molecular Systems Engineering. Further, the Swiss Nanoscience Institute (“Nanoprotect”) is acknowledged and G.G.-G. would like to thank the German Academic Exchange Service (DAAD) r a postdoctoral research fellowship

Can fatty acids and triglycerides rejuvenate bitumen?

S. dos Santos, L.D. Poulikakos, M.N. Partl

[1] *Empa, Swiss Federal Laboratories for Materials Science and Technology, Dübendorf, Switzerland.*

INTRODUCTION: Bitumen occurs in natural asphalt or results from distillation of crude oil. It is composed of 4 main molecular fractions: saturates, asphaltenes, resins and aromatics; e.g. asphaltenes are polyaromatic molecules and paraffinic wax is present in saturates. As bitumen ages, e.g. due to high temperature, it stiffens due to several processes such as oxidation and molecular aggregation. To reutilize bitumen, rejuvenators, e.g. plant oils, are added to it. We investigate the properties of mixtures of bitumen and model rejuvenators such as fatty acids and triglycerides from the rheological point of view. Additionally, we try to understand what happens at the molecular level by studying the phase behaviour of mixtures of asphaltenes, paraffin wax (tetracosane), fatty acids and triglycerides.

METHODS: Rejuvenator – oleic acid, OA, $C_{18}H_{34}O_2$, and triolein, Tri, $C_{57}H_{104}O_6$, (see Fig. 1) – and bitumen or previously aged bitumen at 150 °C for 5 h were weighed at room temperature in the same container and, thereafter, heated at 130 °C for 20 min with intermittent vigorous stirring.

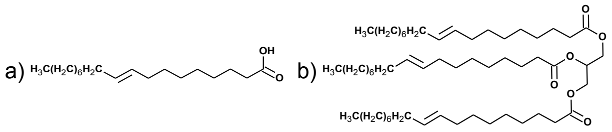

Fig. 1: Oleic acid, OA, a) and triolein, Tri, b).

Bitumen(unaged)-rejuvenator mixtures were also thermally aged after preparation at 150 °C or 180 °C for 5 h. Asphaltenes, tetracosane ($C_{24}H_{50}$), OA and Tri were mixed in toluene and films prepared on glass slides after toluene evaporation.

Oscillatory measurements were performed in a Physica MCR 301 rheometer from Anton Paar (dynamic shear rheometer, DSR) by using plate-plate geometry with 8 mm diameter and gap of 1 mm in the temperature range 0 – 30 °C within the linear viscoelastic region. Master curves of the complex shear modulus, |G*|, were constructed using the time-temperature superposition principle and Williams–Landel–Ferry (WLF) equation fit [1].

RESULTS: Fig. 2a) shows the effect of adding 5 wt% of OA and Tri to aged bitumen and b) shows the effect of ageing bitumen-rejuvenator mixtures.

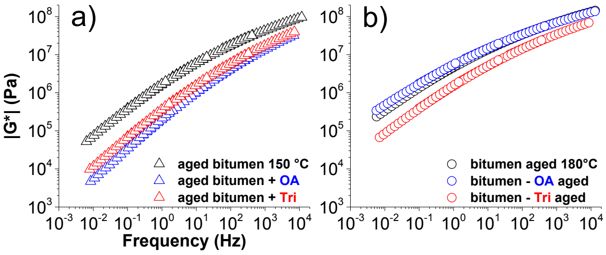

Fig. 2: |G| as a function of frequency of a) aged bitumen mixed with OA and Tri and b) bitumen-OA and bitumen-Tri aged.*

Fig. 2a) shows that the stiffness (i.e. |G*|) decreases by adding OA and Tri to aged bitumen, with larger effect for OA. However, the aged bitumen-Tri mixtures show lower stiffness than aged bitumen-OA mixture, which is at least as stiff as aged bitumen alone (Fig. 2b)). To understand deeper these differences, we study the phase behaviour of mixtures of asphaltenes, paraffin wax (tetracosane), OA and Tri. Fig. 3 shows an example of one thin film after solvent evaporation.

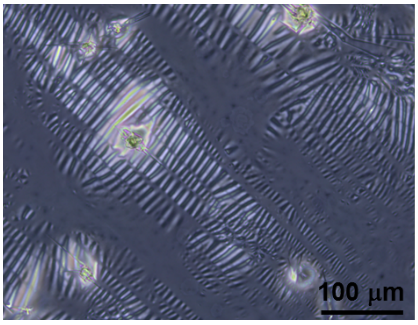

Fig. 3: Optical phase contrast image of film containing asphaltenes, tetracosane and OA.

DISCUSSION & CONCLUSIONS: OA and Tri are able to decrease the stiffness (rejuvenate) of aged bitumen by different extents for the same weight content, being OA more effective. However, when the bitumen-rejuvenator mixture is aged, Tri keeps the rejuvenating property contrary to OA. The phase behaviour of simplified mixtures suggests segregation resulting in patterns resembling spinodal decomposition [2].

REFERENCES: [1] J. D. Ferry; **1980**; *John Wiley & Sons*. [2] de Gennes; **1980**; *J Chem Phys*; 72:4756-4763.

ACKNOWLEDGEMENTS: SNSF 200021 152980/1 and Jakob Heier for helpful discussions.

Particle deswelling and phase behavior of pNIPAM microgels at high concentrations

U. Gasser[1], A. Scotti[1], E.S. Herman[2], M. Pelaez-Fernandez[4], L.A. Lyon[3], A. Fernandez-Nieves[4]

[1] *Laboratory for Neutron Scattering and Imaging, Paul Scherrer Institut, Villigen, Switzerland.*
[2] *School of Chemistry and Biochemistry, Georgia Institute of Technology, Atlanta GA, USA.*
[3] *Chapman University, Schmid College of Science and Technology, Orange CA, USA.*
[4] *School of Physics, Georgia Institute of Technology, Atlanta GA, USA.*

INTRODUCTION: The phase behavior and the particle swelling behavior of concentrated microgel suspensions are not well understood. This is highlighted by the as yet unexplained spon-taneous deswelling of large pNIPAM microgels in a concentrated surrounding of smaller but otherwise identical microgels [1], which allows the suspension to reduce its polydispersity and to crystallize. The interplay of particle-internal degrees of freedom and colloidal degrees of freedom allowing for the spontaneous deswelling is not understood in detail.

METHODS: We have directly observed the deswelling of pNIPAM microgels in concentrated samples at fixed temperature, T~18°C, using small-angle neutron scattering (SANS) with contrast matching. Bidisperse suspensions with a small number of large particles added to a suspension of small particles have been studied. The osmotic pressure in the same samples was determined with a membrane osmometer. Small-angle X-ray scattering (SAXS) was used to determine the phase behavior of bidisperse suspensions with number fractions of large particles between 1% and 70% and also of polydisperse suspensions with polydispersities in the range from 9% up to 20%.

RESULTS: Our SANS measurements show the selective deswelling of the large pNIPAM microgels in bidisperse suspensions with effective volume fractions above a critical value to depend on the fraction of large particles present in the suspension. The osmotic pressure, Π, is found to be compatible with ideal gas behavior at low effective volume fractions ζ□0.8. At higher ζ, the increase of Π becomes significantly steeper. Our SAXS results on bidisperse suspensions reveal a strong dependence of the freezing, ζ_f, and melting, ζ_m, points on the fraction of large particles in the suspension, n_b. Both shift to higher ζ with increasing n_b, and the coexistence regime gets narrower. Crystals are not observed for n_b□0.3. In contrast, polydisperse suspensions are found to have a constant freezing point $\zeta_f \approx 0.67 \pm 0.02$. Crystallization is suppressed for polydispersities > 19%, significantly higher than the 12% limit in hard spheres.

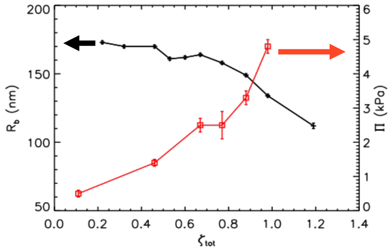

Fig. 1: Particle radius from SANS measurements (black) and osmotic pressure (red) versus effective volume fraction.

DISCUSSION & CONCLUSIONS: Although pNIPAM is an uncharged polymer, pNIPAM microgels carry charged groups on their surface, which are due to the ammonium persulfate starter for the polymerization reaction. Most of the NH_4^+ counterions of the charged groups are trapped close to the microgel surface, but a fraction of them escapes the electrostatic attraction and contributes to the osmotic pressure of the suspension. We find the measured osmotic pressure to be well explained by the free counterions. The counterion clouds of neighboring particles progressively overlap with increasing ζ, leading to an increase of free counterions and the osmotic pressure. This increase of osmotic pressure outside the particles is not compensated by a pressure increase inside the particles and, therefore, the particles deswell when the pressure difference gets larger than their bulk modulus. Large particles are softer than small ones synthesized following the same protocol and, therefore, the larger particles deswell first. We find this model (2) of counterion-induced deswelling to explain both the selective deswelling in bidisperse samples and the "normal" deswelling in monodisperse suspensions. Furthermore, the same model can account for the observed phase behavior in bidisperse and polydisperse pNIPAM suspensions.

REFERENCES: [1] A. St. Iyer and L.A. Lyon, *Angew. Chem. Int.* Ed. 48, 4562-4566 (**2009**). [2] A. Scotti, U. Gasser, E.S. Herman, M. Pelaez-Fernandez, J. Han, A. Menzel, L.A. Lyon, A. Fernandez-Nieves, submitted to PNAS; A. Scotti, *PhD thesis*, ETH Zurich **2015**.

Tailoring Bicelle Morphology and Thermal Stability with Lanthanide-Chelating Cholesterol Derivatives

S.Isabettini[1], E.J.Windhab[1], P.Fischer[1], S.Kuster[1], M.Liebi[2], J.Kohlbrecher[3], T.Ishikawa[4], P.Walde[5]

[1] Laboratory of Food Process Engineering, ETH Zürich, Switzerland. [2] Laboratory for Macromolecules and Bioimaging, [3] Laboratory for Neutron Scattering, [4] Biomolecular Research Laboratory, Paul Scherrer Institute, Villigen, Switzerland. [5] Department of Materials, ETH Zürich

INTRODUCTION: Bicelles composed of DMPC and phospholipids capable of chelating lanthanide ions, such as DMPE-DTPA, are highly tunable magnetic-responsive soft materials [1]. Addition of cholesterol-DTPA conjugates to the bilayer considerably enhances the resulting bicelle's size and magnetic alignability [2]. The high potential of these cholesterol derivatives for bicelle design remains largely unexplored. We examine how molecular structural alterations within the cholesterol-DTPA conjugate leads to contrasting self-assembled polymolecular aggregate structures when incorporated in DMPC/DMPE-DTPA/Tm^{3+} bilayers. The nature of the linker connecting the DTPA-chelating moiety to the sterol backbone is examined by synthesizing chains of various lengths and polarities.

METHODS: Bicelles were prepared as described previously[1]. A total lipid concentration of 15 mM was applied with DMPC/Cholesterol/DTPA-C_n-Cholesterol/DMPE-DTPA/Tm^{3+} (molar ratio 16:2:2:5:7). SANS measurements were conducted at a wavelength of 0.8 nm and a q-range from 0.03 to 1.5 nm^{-1}. DLS measurements were conducted on a Marvern Zetasizer Nano ZS with non-invasive backscatter technology (NIBS) at 5 °C. Cryo-TEM micrographs of the flash-frozen bicelle samples were taken at PSI. The magnetic alignment of the bicelles was quantized at 5 °C and 5.5 T by birefringence measurements.

RESULTS:

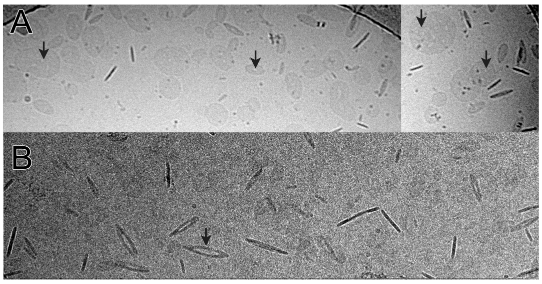

Fig. 1: Cryo-TEM micrographs of DMPC/DMPE-DTPA/Tm^{3+} bicelles containing a 1:1 mixture of cholesterol and DTPA-C_5-Cholesterol flash-frozen at 5 °C (A) and 25 °C (B). Holes in the bicelles are shown with arrows.

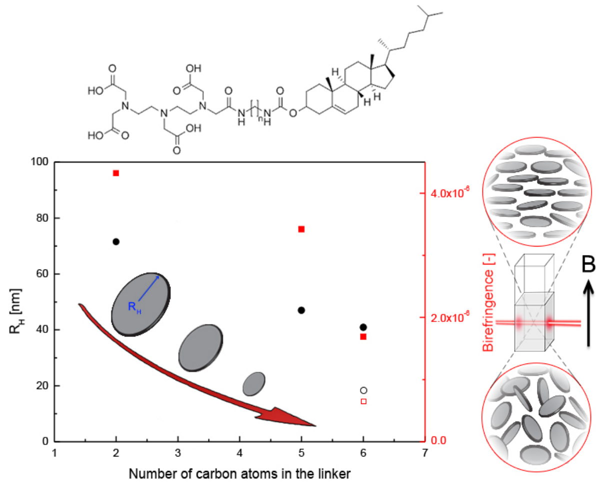

Fig. 2: An inverse correlation exists between the number of carbon atoms in the incorporated Cholesterol-DTPA conjugate's linker and the resulting bicelle's hydrodynamic radius. The magnetic alignability increases with bicelle size as revealed by the birefringence signal.

DISCUSSION & CONCLUSIONS: The increasing degree of freedom for conformational changes conveyed to the chelator head group with increasing linker atomic length reduces the cholesterol-DTPA molecule's critical packing parameter. Consequently, the incorporation of more cone-like molecules in the bilayer favours architectures with higher curvature and results in smaller bicelles. The bicelles' thermo resistivity was greatly enhanced by doping the bilayer with cholesterol-based derivatives. Bicelle structures were maintained up to 40 °C. The versatility of design offered by these amphiphiles engenders new and viable tools for the growing field of magnetically responsive soft materials.

REFERENCES: [1] P. Beck; **2010**; *Langmuir;* 26:5382–5387. [2] M. Liebi; **2013**; *J. Phys. Chem. B.* 117:14743–14748.

ACKNOWLEDGEMENTS: We warmly thank the SNF for funding. C. Holenstein for her contribution to birefringence experiments and the synthesis of the conjugates. Dr. S. Bolisetty for his help with DLS measurements.

Towards a molecular understanding of how vesicles as soft templates regulate and steer enzymatic polymerizations in aqueous media

Sandra Luginbühl, Peter Walde

[1] *Polymer Chemistry, Department of Materials, ETH Zurich, Switzerland*

INTRODUCTION: Sodium bis-(2-ethylhexyl)sulfosuccinate (AOT) vesicles are used as 'soft templates' for the enzymatic oxidation and oligomerization of the aniline dimer, *p*-aminodiphenylamine (PADPA), with *Trametes versicolor* laccase and molecular oxygen to form oligo(PADPA). The products thus formed in the presence of vesicles exhibit a UV-vis-NIR spectrum which is typical for polyaniline in the conductive emeraldine salt form (PANI – ES) – a high absorption in the NIR region. The presence of the vesicles was found to be crucial for the formation of the desired products [1].

METHODS: We attempt to understand the molecular mechanism underlying this 'template effect'. The reactions were conducted with both conventional PADPA and selectively deuterium – labelled PADPA. The resulting products were then extracted and analysed by reverse phase HPLC – MS.

RESULTS: These measurements suggest that there are at least two reaction routes in the presence of vesicles, a major and a minor pathway. The major pathway leads to the formation of a linear aniline tetramer, which is responsible for the high NIR absorption. Without vesicles, the rate of consumption of PADPA is slower, and significant side reactions occur, most prominently hydrolysis, which was determined by using $H_2{}^{18}O$.

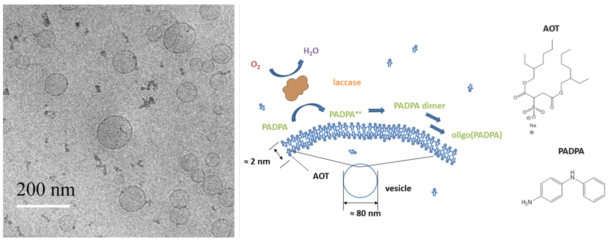

Figure 1: Cryo-TEM image of AOT vesicles (left), schematic illustration of the laccase-catalyzed PADPA oxidation and oligomerization reaction occurring on the surface of vesicles (right).

DISCUSSION & CONCLUSIONS: We propose that that due to the negatively charged surface of the AOT vesicles, there is a high local concentration of PADPA and its oxidation products on or in the hydrophobic membrane, which leads to a faster consumption of PADPA and which promotes the head – to – tail coupling to form the PANI-ES type aniline tetramer. In addition, because PADPA is located in the membrane, it is most likely not surrounded by a lot of water; thus the AOT vesicles protect PADPA and its products from degradation and hydrolysis.

REFERENCES: [1] Junker, K., Luginbühl, S., Schüttel, M., Bertschi, L., Kissner, R., Schuler, L.D., Rakvin, B., Walde, P., *ACS Catalysis,* **2014**, 4, 3421

ACKNOWLEDGEMENTS: We thank Louis Bertschi, MS Service Lab, LOC, ETHZ for his support in the ESI – MS measurements; Dr. Takashi Ishikawa, PSI, for the Cryo-TEM measurements; Swiss National Science Foundation (SNF).

Facile synthesis of self-healing microcapsules

D. G. Moore[1], J. Brignoli[2], T. Moser[1], A. R. Studart[1]

[1] ETH Zürich, Zürich, Switzerland. [2] EPFL Lausanne, Lausanne, Switzerland

INTRODUCTION: In nature biological materials self-heal and adapt repeatedly to stresses caused by the environment. For instance in bone, the osteocytes, osteoblasts, and osteoclasts each respond to chemical and mechanical input in order to remodel bone to better suit physical loading [1]. So far, major efforts have been made to create engineered microcapsules that can, upon rupturing, release a healing agent. Such self-healing materials only have a partial recovery of the strength and the self-healing ability is depleted after the capsule ruptures a single time. To mimic the dynamic biological function, we created functional microcapsules that release self-healing agents, but may also themselves be healed, allowing for multiple release events. Currently there are many limitations in synthesizing microcapsules with self-healing polymer shells. We address these challenges with a strategy by combining two orthogonal, self-setting, polymer components that form a double network in-situ. In order for a microstructure such as a microcapsule to self-heal it is important that the polymer has some elastic recovery to return to its original shape, but also has a self-healing agent that can diffuse through the crack boundary [2]. In this project we present a double network polymer that consists of one elastic network and one self-healing network.

METHODS: We use a microfluidic approach to produce w/o/w emulsions as a template for microcapsules [3], where the polymer components are in the oil phase. The self-healing network consists of zinc neutralized poly(butyl acrylate-co-acrylic acid) ionomer [4] and the elastic network consists of a trimethoxysilane functionalized Jeffamine, which forms a network through polyoctahedral silsesquioxane crosslinking. Both materials are soluble in oil and set by the diffusion of oil away from the capsule and water into the capsule. Because of this, oils such as dichloromethane and toluene, which diffuse through water readily, are ideal solvents for the oil phase. Setting of the capsule shells occurs over night with no intervention resulting in double network polymer shells.

RESULTS: Polymer components were synthesized in advance of the microcapsule preparation. Polymers were investigated in bulk through rheometry and FTIR. The degree of ionic crosslinking was varied in the ionomer and, predictably, showed increasing elasticity with increasing concentration of ionic crosslinking sites. The effect of molecular weight and number of functional groups of the trimethoxysilane modified Jeffamine was also investigated. Finally microcapsules were formed.

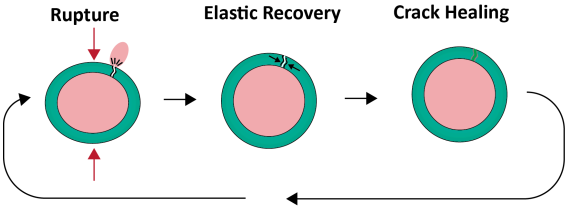

Fig. 1: Multiple release from a microcapsule requires elastic recovery, followed by crack healing of the polymer shell. These separate events can be individually handled by the two components of a double network polymer.

DISCUSSION & CONCLUSIONS: In an effort to mimic the cellular components responsible for the adaptive remodeling of bone, microcapsules capable of multiple-release were synthesized. Multiple-release was achieved by using a self-healing polymer shell. Most self-healing materials are not suitable for the emulsion template method normally used to make microcapsules. Because of this, a novel polymer double network was tested in which both oil soluble polymers orthogonally set in the presence of water. These multiple-release microcapsules may enable the development of adaptive materials, which strengthen in response to loading, rather than simply repairing.

REFERENCES: [1] A. R. Studart, *Angew. Chem. Int. Ed. Engl.*, vol. 54, no. 11, pp. 3400–3416, Mar. **2015**. [2] X. Luo and P. T. Mather, *ACS Macro Lett.*, **2013**. [3] A. S. Utada, E. Lorenceau, D. R. Link, P. D. Kaplan, H. A. Stone, and D. A. Weitz, *Science*, vol. 308, no. 5721, pp. 537–541, Apr. **2005**. [4] R. K. Bose, N. Hohlbein, S. J. Garcia, A. M. Schmidt, and S. van der Zwaag, *Phys Chem Chem Phys*, vol. 17, no. 3, pp. 1697–1704, Jan. **2015**.

ACKNOWLEDGEMENTS: This research was funded by the NCCR for Bio-Inspired Materials.

Determining elastic moduli of interfacial films with a pendant drop apparatus

M. Nagel[1], M. Pepicelli[1], C. Trégouët[2], C. Monteux[2] & J. Vermant[1]

[1] ETH Zürich, Zürich, Switzerland. [2] ESPCI, Paris, France.

INTRODUCTION: We present a novel algorithm that allows to determine elastic shear and dilatation moduli from pendant drop images. The method is verified on computer-generated images and then applied to a viscoelastic polymer whose properties have been measured with a Langmuir trough.

METHODS: A single layer of PVP and PMAA is assembled by hydrogen bonds on a liquid interface[4]. On a self-made pendant drop device the drop volume is oscillated and the drop shape recorded. Whereas the surface tension in most interfaces is uniform and acts isotropic the interface with the polymer network exhibits deviatoric stresses and is thus neither uniform nor isotropic.
Several approaches to study anisotropic interfaces on a pendant drop device have been proposed recently in the literature [1,2,3]. In our approach we formulate the problem with a novel implicit scheme, which leads to an over-determined system of equations, instead of fitting the acquired shape to a solution of an explicit shooting method. In minimizing the error of the over-determined problem we obtain a fit with increased robustness.

RESULTS: At first we verify the method on a simulated interface with known surface tension and elastic moduli. The parameters can be retrieved with great precision if the coordinates are used directly (not shown).

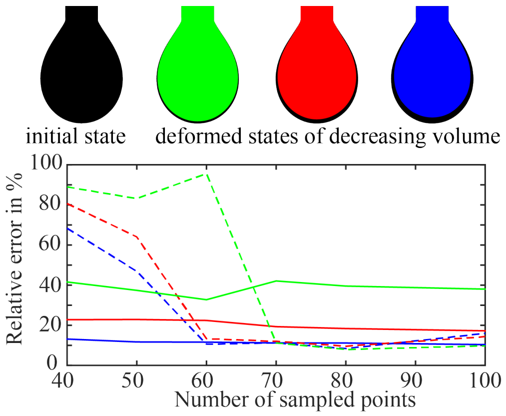

Fig. 1: Relative error when fitting marginally oscillated drops. Smaller deformation = larger error.

In order to check the robustness against noise the simulated coordinates are converted into images and then read into the acquisition and fitting algorithm. Figure 1 shows 4 different drop shapes and the convergence of the method depending on the number of sampled points and the compression.

Figure 2 shows a sequence of images of the drop with PVP-PMAA interface. The dilatation and shear modulus are plotted for several images while the interface is compressed.

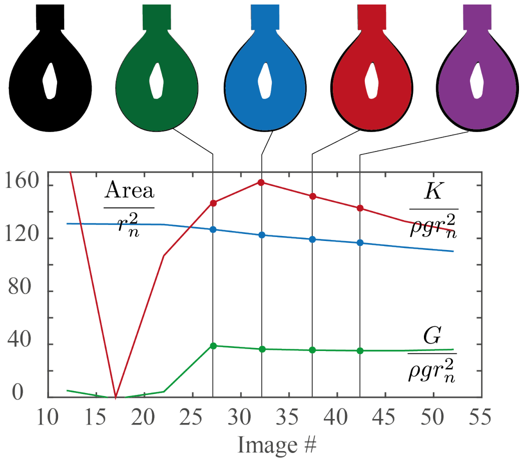

Fig. 2: Shear modulus (G) and dilatation modulus (K) for a compressed drop. Early frames show larger errors; later frames may exhibit relaxing behaviour.

DISCUSSION & CONCLUSIONS: Due to the nonlinear character of the underlying problem the error can become arbitrarily large depending on the operation conditions, as the effect of elasticity on the drop shape appears in combination with surface tension. A minimum compression is needed before consistent data can be obtained. The decaying moduli in Figure 2 might indicate a viscous behaviour and points out the utility of being able to fit a pair of consecutive images and not a pair of isotropic and compressed state images. The dependency of the fitting on an isotropic reference state has been pointed out as one major limitation of the method [3]. Currently we are working on a generalization of the method in order to retrieve material information that is independent of an isotropic reference state.

REFERENCES: [1] D. Carvajal et al. *Softmatter* 7 (22) **2011**; [2] S. Knoche et al. *Langmuir* 29 (40) **2013**; [3] K.D. Danov et al. *JCIS* 440 **2015;** [4] Le Trilly et al. *ACS Macro Letters* **2015**.

Tuning structural relaxations of strongly correlated colloidal systems

Nazzani F., Trappe V.*

University of Fribourg, Department of Physics, Chemin du Musée 3, Fribourg, Switzerland

* Corresponding author: veronique.trappe@unifr.ch

INTRODUCTION: The relevant parameter governing the glass transition of colloidal systems is in general the particle concentration. In this contribution we explore the glass transition of charged microgels at quasi-deionized conditions, varying the particle number concentration of a given microgel system (M1) by a) dilution with water and b) addition of a less charged microgel system (M2).

RESULTS & DISCUSSION: Remarkably, we find that the structural relaxation time of our original system decreases less upon dilution with water than upon addition of the less charged microgel system. This is shown in Figure 1, where we report the alpha relaxations obtained for both series as a function of the number concentration of the more highly charged microgels M1. Let us stress that the total particle number concentration $N_{tot} = N_{M1} + N_{M2}$ is constant in series b), while $N_{M1} = N_{tot}$ in series a).

Clearly, the particle number concentration is not the only parameter governing the dynamics. The introduction of defects is very efficient in releasing the constraints governing slow dynamics. Indeed, using the magnitude of the nearest neighbour peak of the static structure factor $S(q_{peak})$ as a measure of the degree of correlation in particle position, we find that the degree of correlation remains very high when diluting with water, while introducing defects leads to a significant loss of correlation, as shown in Fig. 2. Such loss in correlation directly impacts the structural relaxation process.

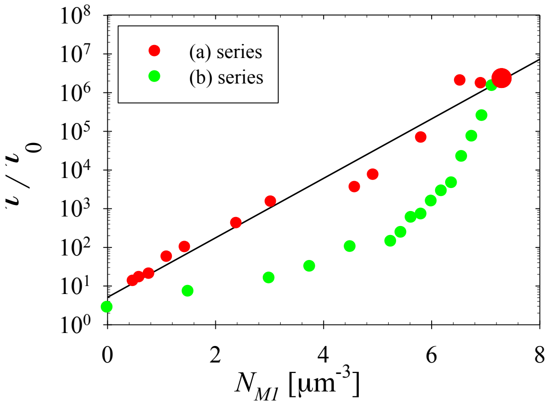

Fig. 1: Structural-relaxation time τ_α normalized by the free diffusion time τ_0 as a function of the number concentration of M1.

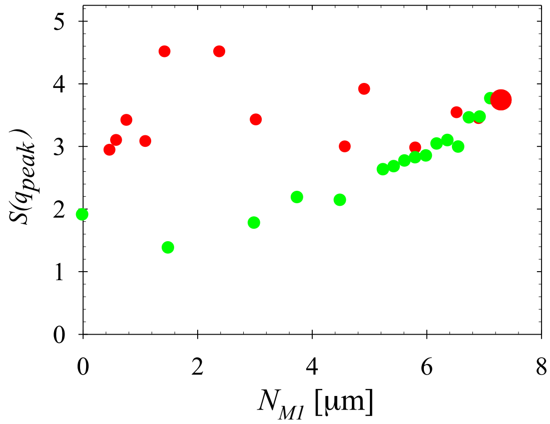

Fig. 2: Magnitude of the structure factor at the nearest neighbour peak as a function of N_{M1}.

Particle-level simulations and shear rheometry in hybrid magnetic/non-magnetic suspensions

E.M. Ortigosa-Moya, J.A. Ruiz-López and J. de Vicente

Biocolloid and Fluid Physics Group, Department of Applied Physics, Faculty of Sciences,
University of Granada, C/Fuentenueva s/n, 18071 - Granada, Spain

jvicente@ugr.es

Under particular circumstances, magnetized suspensions of ferromagnetic micronsized particles in a liquid carrier exhibit an apparent yield stress due to the formation of field-induced structures in the field direction. This is the so-called magnetorheological (MR) effect. Interestingly, recent experimental works demonstrate a dramatic enhancement in the MR performance of hybrid magnetic colloids formulated by partial substitution of magnetic particles by non-magnetic particles. However, the mechanism behind this MR enhancement is still unknown.

Here, a Brownian-dynamic simulation study is proposed to get a better insight. The simulations take into account both hydrodynamic interactions and frictional/contact forces between the particles. Hence, both translational and rotational motion of the particles are solved. Simulations are then compared with MR experiments using stress-controlled rheometers (Anton Paar MCR 302 and MCR 501) on model suspensions constituted by carbonyl iron as the magnetic phase and either starch (30-42 vol%) or fumed silica (5-25 vol%) in Newtonian carriers.

REFERENCES: [1] Ulicny J C, Snavely K S, Golden M A and Klingenberg D J (**2010**) Enhancing magnetorheology with nonmagnetizable particles, *Applied Physics Letters*, 96, 231903. [2] Bombard A J F, Gonçalves F R, Morillas J R and de Vicente J (**2014**) Magnetorheology of Dimorphic Magnetorheological Fluids based on Nanofibers, *Smart Materials and Structures*, 23, 125013.

ACKNOWLEDGEMENTS: This work was supported by MINECO MAT 2013-44429-R and PCIN-2015-051 projects (Spain), European Regional Development Fund (ERDF) and by Junta de Andalucía P10-RNM-6630 and P11-FQM-7074 projects (Spain). E.M.O.M. acknowledges financial support provided by the MINECO through "Ayudas predoctorales para la formación de doctores 2014" (BES-2014-069341). J.A.R.-L. acknowledges financial support by the "Ministerio de Educación: Becas del Programa de Formación del Profesorado Universitario (FPU)" (AP2010-2144).

Interaction of potato starch paste and sugar by fractional rheological model

M. Orczykowska, P. Owczarz, M. Dziubiński, A. Rył

Lodz University of Technology, Department of Chemical Engineering, Lodz, Poland.

INTRODUCTION: The best known polysaccharide is starch. Due to industrial importance of starch used in fruit and vegetable industry, confectionery and meat processing, the rheological properties of starch pastes are a subject of continuous studies. Due to a relatively low stability of pure starch pastes and the impact of many factors on their rheological properties, a number of additives in the form of non-starch polysaccharide hydrocolloids, such as gum arabic, guar gum or xanthan gum are commonly used to control the process of starch paste formation. However, starch pastes are now frequently stabilized by means of carbohydrates.

METHODS: It is indicated that the structure can be assessed during the interaction of potato starch paste and carbohydrate using a rheological fractional standard linear solid model. A standard linear solid model [1] is composed of a spring and a system of elements of the Maxwell model, i.e. the spring connected in series with a dashpot in which the dashpot and spring are replaced by the Scott-Blair element called a viscoelastic element – a springpot – see Fig. 1. The advantage of the fractional rheological models is that it can describe dynamic behaviour by means of a single equation which contains a number of constant parameters determining viscoelastic properties of the tested material – see equation (1):

$$G^*(\omega) = G_e + G_0 \cdot \frac{(i\omega\tau_0)^{\alpha}}{1 + (i\omega\tau_0)^{\alpha-\beta}} \qquad (1)$$

The value of an equilibrium modulus, modulus of elasticity in the steady state flow condition G_e, represents total elasticity of the network. The value of viscoelastic modulus of plateau G_0 is identified with cross-linking power of the structure. The value of characteristic relaxation time τ_0 defines the time after which stress relaxation will occur. Short relaxation times indicate strong elastic properties of the material. The values of parameters α and β indicates a characteristic behaviour of elastic bodies if its value is equal to zero; when it is equal to one the behaviour is characteristic of viscous liquids. As a result, rheological parameters from equation (1) are used in a comprehensive analysis of viscoelastic properties of the tested material.

RESULTS: The analysis of data obtained by means of the fractional rheological model allowed us to state that for potato starch paste and a mixture of this paste with sugar a medium is formed with a structure representing the behaviour typical of viscoelastic quasi-solid bodies – high values of the viscoelastic modulus of plateau G_0. Addition of carbohydrate to the fresh potato starch paste caused a increase of the value of equilibrium modulus G_e responsible for the total network elasticity. But in the case of potato starch paste after 24 hours in ice box in temperature 5^0C the value of equilibrium modulus G_e decreased. The values of fractional exponents α and β and characteristic relaxation time τ_0 indicate strong elasticity of potato starch pastes and carbohydrate composites.

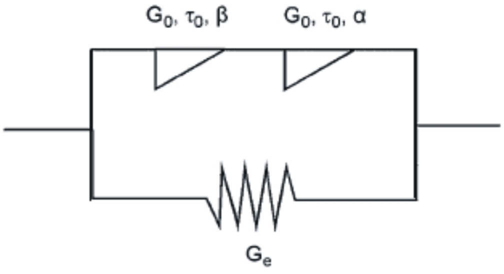

Fig. 1: Standard linear solid model (SLSM) – fractional rheological Zener model with two springpots.

DISCUSSION & CONCLUSIONS: It was proved in this study that fractional rheological model in the description of biomaterial structure could be used to carry out a comprehensive analysis and estimation of structural properties of the material, including viscous, elastic or viscoelastic properties. The fractional rheological models provide much more information on the structure of biomaterials than the previously applied classical mechanical Maxwell or Kelvin-Voigt models. Analysis of the data obtained by means of the Zener fractional rheological model led to a conclusion that pastes produced from potato starch with and without carbohydrates are the media with a structure behaving in a way typical of viscoelastic quasi-solid bodies.

REFERENCES: [1] H. Ma et al.; **2011**; *Macromol. Chem. Phys.;* 212:252-258.

Recent advances in DWS microrheology

Mathias Reufer, Frédéric Mondiot; Magdalena Priebe; Andreas Charles Völker

INTRODUCTION: Diffusing Wave Spectroscopy (DWS) is an optical microrheology technique that has been applied successfully to several colloidal model systems, such as gels, suspensions, polymer solutions, emulsions and foams. It is a fast and noninvasive technique where the sample dynamics can be probed down to sub-nanometer resolution at high frequencies.

The contact free nature of DWS microrheology ensures that data is collected exclusively within the linear viscoelastic regime. However, by applying the Cox-Merz rule also non-linear behavior can be predicted. This is particularly interesting because DWS microrheology covers high frequencies, which corresponds to high shear rate that can not be covered by conventional rheometers.

RESULTS & DISCUSSION: We present studies on polymer solutions and silicon oils where DWS microrheology is combined with conventional rheology. In particular, we show how the Cox-Merz rule can be applied to extend the measurement range of a flow curve to very high apparent shear rates. This combined approach opens the route for measurements over a range of shear rates that spans over several orders of magnitude.

Particle Sizing - Recent advances in DLS technology

N.B.Kambly[1], A. Vaccaro[1], M. Reufer[1], A.C.Voelker[1]

[1] *LS Instruments, Fribourg, Switzerland (* http://www.lsinstruments.ch *)*

nils.kambly@lsinstruments.ch

Dynamic light scattering (DLS) is probably the most common technique to analyze the size of suspended particles with sizes in the range from nanometer to micrometer. DLS can be applied to a variety of systems such as nanoparticles, polymers, proteins, peptides, and emulsions. The working principle of DLS particle sizing is the analysis of the intensity fluctuations of scattered light caused by the random Brownian movement of the particles. Based on the correlation function of the scattered light intensity one can determine the diffusion coefficient of the particles. If the temperature and the viscosity of the sample are known, the particle size and size distribution can be determined. Since the DLS analysis is based on the assumption that only singly scattered light is detected, multiple scattering of light results in an inaccurate measure of the particle size leading to significant underestimations of the hydrodynamic radius. In practice, this means that samples need to be diluted prior to the DLS measurement in order to avoid multiple scattering. However, it is often difficult to find the optimal degree of dilution while retaining a sufficient light scattering signal. The contamination of the DLS signal by multiple scattering is thus making an accurate DLS more cumbersome. Moreover, it is limiting the application range of DLS to systems that do not suffer from dilution, which is not always the case. Two alternative strategies to dilution can be adopted with the aim to increase the range of application of DLS to higher sample concentrations. First, multiple scattering can be minimized by reducing the optical path of the laser beam in the sample. Second, multiple scattering can be suppressed actively. A combination of both strategies gives access to the highest measurable sample concentrations. Today the most powerful technique to suppress multiple light scattering is based on the "3D crosscorrelation" principle, which we recently improved further with the "modulated" 3D technology. As we will demonstrate, the performance of this technique can be further increased when combined it with path length reduction techniques. This leads to a substantially increased sensitivity, which results in both smaller measurable nanoparticle sizes and an increase of the measurable sample concentrations. Here we present first results and give an outlook to further developments.

REFERENCES: [1] Patent EP2365313 A1. [2] Modulated 3D cross-correlation light scattering: Improving turbid sample characterization, Ian D. Block and Frank Scheffold, *Rev. Sci. Instrum*. 81, 123107 (**2010**).

Colloidal binary monolayers under oscillatory shear at liquid-liquid interfaces

Hendrik Th. Spanke[1], Ivo Buttinoni[1], Lucio Isa [1]

[1] *ETH Zürich, Zürich, Switzerland.*

INTRODUCTION: Colloidal systems allow the simultaneous measurement of their macroscopic response to shear and deformation and observation of the microscopic structural evolution. Using an active microrheology setup described by Zell et al. [1], Buttinoni et al. [2] investigated the response of colloidal binary mixtures under steady shear. We extend this work to oscillatory shear. With a Boussinesq number well above 1, this technique accesses the interface-dominated regime of rheological properties.

METHODS: We produced glassy colloidal binary monolayers with area fractions upwards of 10% and ratios of small (d=1.1 μm) to big Polystyrene particles (d=2.8 μm) between 1:2 and 2:1. With increasing amplitude of the oscillation and fixed frequency of 0.1 or 0.5 Hz,

RESULTS & DISCUSSION: we observe the small particles yielding and plastically rearranging before the big particles. This is shown by calculating the root mean square displacement (RMSD) of the particles between individual oscillation cycles. By looking at these RMSD values versus the local strain, it is possible to determine the exact strain, at which the particles yield.

CONCLUSIONS: To gain a more complete picture of the exact onset of plasticity as a function of frequency and amplitude of the oscillation as well as the area fraction and particle number ratio, more experiments are needed at higher frequencies. Here the system is expected to transition to a solid like, elastic behavior. Furthermore, by tuning the particle number ratio and achieving a homogeneous distribution of the two particle sizes in the system, it is possible to investigate the microscopic response of alloy structures to applied shear.

REFERENCES: [1] Zell, Zachary A. and Mansard, Vincent and Wright, Jeremy and Kim, KyuHan and Choi, Siyoung Q. and Squires, Todd M., *Linear and nonlinear microrheometry of small samples and interfaces using microfabricated probes, Journal of Rheology*, 60, 141-159 (**2016**). [2] I. Buttinoni, Z. A. Zell, T. M. Squires, and L.Isa., *Colloidal binary mixtures at fluid-fluid interfaces under steady shear: structural, dynamical and mechanical response*, *Soft Matter.* **2015** Nov 14; 11(42):8313-21

SIMULATIONS OF A HEAVY BALL FALLING THROUGH A SHEARED SUSPENSION

A. K. Townsend[1], H. J. Wilson[1]

[1] *University College London, London, UK.*

INTRODUCTION: Blanc and coworkers [1] recently discovered that a heavy ball falling through a dense suspension of smaller particles can be made to fall much faster by applying a transverse oscillatory shear to the system, as in geometry **[A]** of Fig. 1. The mechanism, they hypothesise, is all in the microstructure created in the small-particle suspension by each flow. A falling ball creates an asymmetric density disturbance, with more particles ahead of it than are found in its wake; this naturally hinders its falling. The cross-shear, on the other hand, may encourage the small particles to align in the vertical direction, making it easier for the large sphere to pass.

They also found that for very concentrated suspensions (a volume concentration of $\phi = 0.47$), if they tracked the large ball's fall speed during a shear oscillation, its variation was so extreme that at some moments of the shear cycle it was actually travelling upwards. In this paper we aim to reproduce some of these observations numerically, and therefore elucidate the importance of various physical parameters on the two phenomena.

METHODS: We model these experiments using a Stokesian Dynamics simulation, written in Python. We show how the motion of the heavy particle depends on two key dimensionless parameters: the frequency of the oscillations (relative to a typical settling time) and the strength of repulsive interparticle forces, such as DLVO, relative to the buoyancy-adjusted weight of the heavy ball.

Geometries **[B]** and **[C]** in Fig. 1 show two other possible orientations of the shearing flow relative to the fall direction. Preliminary results for a layer in geometry **[B]** are presented below.

PRELIMINARY RESULTS: In Fig. 2 we show the transient fall speed (normalised by the Stokes velocity of the large sphere in pure solvent) during a single oscillation of the shear flow for four different parameter combinations with the ball falling in the flow gradient direction **[B]**. The system is first presheared for two oscillations before the ball begins to fall; we show the second falling oscillation here.

We find that a change in the magnitude of the repulsive force has only a weak effect on the mean velocity, but that a higher frequency can increase mean velocity by 10%.

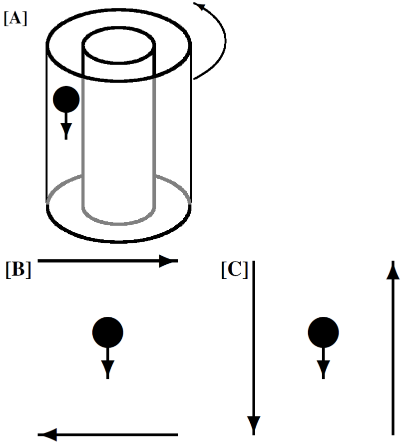

Fig. 1: Three different possible orientations of the fall direction relative to the oscillatory shear flow. **[A]** *Vorticity direction, as in the Couette device experiments of* [1]*;* **[B]** *Flow gradient direction, as reported here;* **[C]** *Flow direction.*

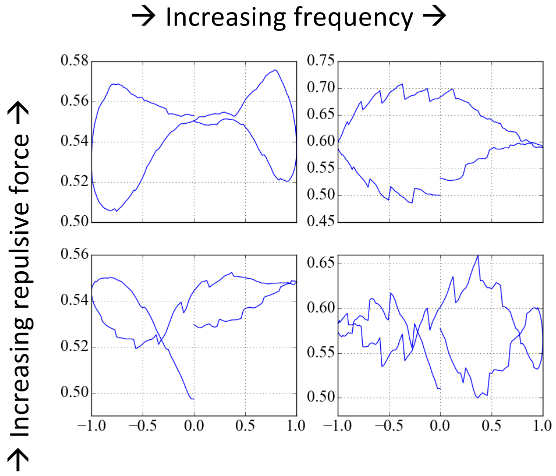

Fig. 2: 2D simulations of a ball falling in the flow-gradient direction (geometry **[B]** *of Fig. 1). We plot the instantaneous fall speed v against state of shear. In each plot, the oscillation begins with motion to the right.*

REFERENCES: [1] F. Blanc, E. Lemaire, F. Peters; **2014**; *J. Fluid Mech*; 746:R4

Simultaneous Optical and Electrochemical Characterization of Voltage Sensitive Dyes in Lipid Membranes

Maria Tsemperouli, Kaori Sugihara

Department of Physical Chemistry, University of Geneva, Geneva, Switzerland.

INTRODUCTION: Voltage sensitive dyes (VSDs) are powerful tools for cell membrane potential monitoring. The main characteristic of VSDs is the change in their inherent fluorescence upon membrane potential changes. The characterization of VSDs is commonly performed either directly with living cells or with vesicles where the membrane potential is established by incorporating ion selective channels. However, both characterization methods lack the possibility to precisely control the voltage sequences, thus are unable to study the kinetics of the dyes. In this work, a new approach for the mechanistic and kinetics studies of VSDs in lipid membranes is proposed.

METHODS: First, pores (φ = 1 µm) were fabricated in silicon nitride thin (200 nm) membranes by focused ion beam (FIB). Second, the membrane with pores was mounted in a home-made electrochemical cell where both sides of the membrane are electrically accessible. Third, free-standing lipid bilayers were formed over the pores either by preparation of black lipid membranes (BLMs) or by giant unilamellar vesicle (GUV) rupture. After the incorporation of VSDs (*e.g.* di-4-ANEPPS), the fluorescence signal from the bilayer is monitored by fluorescence microscopy while applying different voltage sequences with a four electrode system.

RESULTS & DISCUSSION:

Free-standing lipid bilayer: We performed electrochemical impedance spectroscopy experiments to electrically characterize the pored substrate. Fig. 1 shows the impedance changes of the pored Si3N4 membrane before and after the lipid bilayer formation via painting of lipids in decane (BLMs). Pore spanning lipid bilayers formed by GUV rupture are more fragile and rupture easily making electrophysiology experiments impossible. To face the bad stability effect further chemical functionalization of the pored Si3N4 membrane is required, an experimental step which is still under current optimization.

Voltage-dependent Fluorescence of di-4-ANEPPS: The electrochromic dye di-4-ANEPPS appears a voltage-dependent shift in the excitation or emission spectrum where the dye is assumed to be bound to the extracellular surface of the membrane and undergo charge distribution in its excited state. The magnitude of the spectral shift is linearly related to the change in the potential.

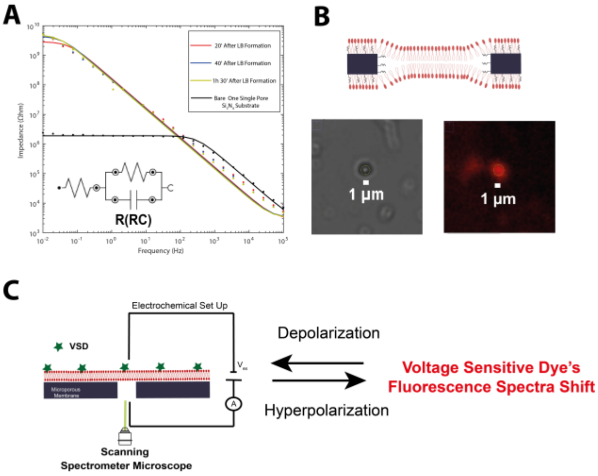

Fig. 1: Electrochemical impedance spectrum of one single pore with and without lipid bilayer (A). Schematic BLM formation on one single pore Si_3N_4 membrane and fluorescence image was taken to validate the BLM formation (B). Schematic representation of the whole experimental set up for VSDs' response studies (C).

CONCLUSIONS: The proposed platform offers the possibility 1) to apply any voltage sequences, 2) to modify bilayer composition freely, and 3) to acquire two-dimensional mapping of the VSD activities, allowing more detailed studies of VSDs.

REFERENCES: [1] K. Sugihara, J. Vörös, T. Zambelli, *ACS Nano* 4, 5047-5054 (**2010**), [2] Kocun, M.; Lazzara, T. D.,; Steinem, C., Janshoff, A. *Langmuir* 27, 7672 (**2011**), [3] V. Montana, D. L. Farkas, L.M. Loew, *Biochemistry* 28, 4536-4539 (**1989**)

ACKNOWLEDGEMENTS: This work is supported by the Swiss National Centre of Competence in Research., NCCR Chemical Biology. We also thank the staff of Center of Micronanotechnology CMI of EPFL in Lausanne for the access to microfabrication facilities.

The effect of the heat rate and pH on the kinetics of sol-gel phase transition for chitosan hydrogel systems.

P. Owczarz[1], Z. Modrzejewska[1], P. Ziółkowski[1], A. Skwarczyńska[2], A. Bartkowiak[3], M. Dziubiński[1]

[1] Lodz University of Technology, Lodz, Poland. [2] Rzeszow University of Technology, Rzeszow, Poland. [3] West Pomeranian University of Technology, Szczecin, Poland

INTRODUCTION: Chitosan is a semi-crystalline amino polysaccharide, slightly soluble in water, obtained by deacetylation of chitin. A low concentrated acid solutions are used as a solvent. Under acidic conditions, ion H^+ is bound to the amino group $-NH_2$ in polysaccharide ring. Therefore, hydrophilic properties of chitosan are being to predominate over hydrophobic properties and results in the formation of a colloidal system in which the polymer chains are dispersed in continuous phase - acid solution. Such a colloidal system is sensitive to temperature and/or pH changes. Under effect of temperature increase (at constant pH), sol-gel phase transition occurs. The temperature increase causes a reduction in the dissociation degree of amino group $–NH_3^+$ and therefore a loss of hydrophilic properties of the chitosan chains. Chitosan and water particles are no longer attracted to each other and the cross-linked structures are begin to form. The use of an acid as a solvent causes that the value of chitosan solution pH is significantly below 7 and the temperature of phase transition exceeds 37°C. Therefore it is necessary to add alkaline compound to the solution which results in pH increases to neutral value and thus change the electrokinetic interactions between the polymer chains and solvent. The temperature of phase transitions decreases and for pH value of 7 fluctuates around 37°C.

METHODS: The paper presents study of the impact of temperature and its increase on the temperature of phase transition for a chitosan thermosensitive systems. Low-concentrated chitosan solutions in 0,1 M HCl with different molecular weight but the same deacetylation degree were taken as a measurement samples. The experiments were performed for acidic solutions of chitosan, and for systems containing additionally disodium β-Glycerophosphate (NaGP) to increase pH value. Measurements of the rheological properties under isothermal conditions and effect of temperature increase were performed. Measurement of zeta potential changes was also performed. SEM pictures of hydrogel structure after freeze-drying were made.

RESULTS: Based on rheological and zeta potential measurements, the phase transition temperature under effect of temperature increase for chitosan systems was determined. Obtained results are compared with gels classification method - based on course of oscillatory spectra - proposed by Zaccone *et al.* [1]. Rheological curves have demonstrated that hydrogel structure formation from solution of chitosan and HCl is possible. However, in that case the phase transition temperature is substantially higher compared with system containing additionally NaGP. SEM pictures analysis of gels formed from solutions containing NaGP revealed the presence of NaCl crystals in the resulting hydrogel structure. Obtained results are in accordance with the theory of ion H^+ transfer between chitosan and NaGP molecules, which was presented by Lavertu *et al.* [2].

DISCUSSION & CONCLUSIONS: Hydrogel composed of low-concentrated acidic solutions of chitosan is classified as physical gel. Although the kinetic of its formation is limited by chemical change as well as a physical change. The chemical changes are related with reduction of chitosan pK_a induced by thermal energy (release of proton from chitosan molecule $-NH_3^+ \leftrightarrow -NH_2 + H^+$). Whereas, the physical changes are related with increase of the diffusion coefficient of the polymer solution - which follows from decrease in viscosity with temperature increase.

REFERENCES: [1] A. Zaccone, H.H. Winter, M. Siebenbürger, M. Ballauff; **2014**; *Journal of Rheology*; 58: 1219-1243. [2] M. Lavertu, D. Filion, M.D. Buschmann; **2008**; *Biomacromolecules*; 9: 640–650.

ACKNOWLEDGEMENTS: The research was financed by the National Science Center of Poland – Grants NCN UMO-2011/01/B/ST8/06686 and continued NCN UMO-2014/15/B/ST8/02512.

Participants

Mrs.	Lauriane	Alison	ETH Zurich	Switzerland	lauriane.alison@mat.ethz.ch
Dr.	Oleg	Aseev	University of Zurich	Switzerland	oleg.aseev@uzh.ch
Mr.	Victoria	Blair	ETH Zurich	Switzerland	victoria.blair@mat.ethz.ch
Mr.	André	Brem	ETH Zurich	Switzerland	andre.brem@mat.ethz.ch
Dr.	Ivo	Buttinoni	ETH Zurich	Switzerland	ivo.buttinoni@mat.ethz.ch
Dr.	Anja	Car	University of Maribor	Slovenia	anja.car@unibas.ch
Mrs.	Jui-Chia	Chang	EPFL	Switzerland	jui-chia.chang@epfl.ch
Dr.	Gabriele	Colombo	ETH Zurich	Switzerland	gabriele.colombo@mat.ethz.ch
Dr.	Gaurasundar	Conley	University of Fribourg	Switzerland	marc.conley@unifr.ch
Mrs.	Alice	Cont	EPFL	Switzerland	alice.cont@epfl.ch
Mr.	Salvatore	Costanzo	Foundation for Research and Technology - Hellas (FORTH)	Greece	salvcost@iesl.forth.gr
Dr.	Ahmet	Demiroers	ETH Zurich	Switzerland	ahmet.demiroers@mat.ethz.ch
Mrs.	Yuanyuan	Deng	ETH Zurich	Switzerland	ydeng@student.ethz.ch
Mr.	Sven	Deutschländer	University of Zurich	Switzerland	sven.deutschlaender@uzh.ch
Mr.	Kilian	Dietrich	ETH Zurich	Switzerland	kilian.dietrich@mat.ethz.ch
Dr.	Salomé	dos Santos	Empa, Swiss Federal Laboratories for Materials Science and Technology	Switzerland	
Prof.	Eric	Dufresne	ETH Zurich	Switzerland	ericd@ethz.ch
Prof.	Marek	Dziubinski	Lodz University of Technology	Poland	marek.dziubinski@p.lodz.pl
Mr.	Tomaz	Einfalt	University Basel	Switzerland	tomaz.einfalt@unibas.ch
Dr.	Jan	Engmann	Nestlé Research Center		jan.engmann@rdls.nestle.com
Mrs.	Anubha	Garg	ETH Zurich	Switzerland	anubha.garg@hest.ethz.ch
Dr.	Urs	Gasser	Paul Scherrer Institut	Switzerland	urs.gasser@psi.ch
Mrs.	Danila	Gaudino	University of Naples	Italy	danila.gaudino@unina.it

			Federico II		
Dr.	Saroj	Ghimire		Switzerland	masaroj@gmail.com
Dr.	Deniz	Gunes	Nestlé		zeyneldeniz.gunes@rdls.nestle.com
Dr.	Ilja	Gunkel		Switzerland	ilja.gunkel@unifr.ch
Mrs.	Zahraalsadat	Hejazi	EPFL	Switzerland	zahraalsadat.hejazi@epfl.ch
Mr.	Chiao-Peng	Hsu	ETH Zurich	Switzerland	chsu@student.ethz.ch
Prof.	Kyu	Hyun	Pusan National University	South Korea	kyuhyun@pusan.ac.kr
Dr.	Lucio	Isa	ETH Zurich	Switzerland	lucio.isa@mat.ethz.ch
Mr.	Stéphane	Isabettini	ETH Zürich	Switzerland	stephane.isabettini@hest.ethz.ch
Mr.	Alan	Jacob	IESL, Foundation of Research and Technology/University of Crete	Greece	alanjacob88@yahoo.com
Mr.	Etienne	Jeoffroy	Empa / ETH Zürich	Switzerland	etienne.jeoffroy@mat.ethz.ch
Prof.	Ju Min	Kim	Ajou University	South Korea	jumin@ajou.ac.kr
Dr.	Joachim	Kohlbrecher	Paul Scherrer Institut	Switzerland	joachim.kohlbrecher@psi.ch
Mrs.	Yuly	Lopez	ETH Zurich	Switzerland	yulyl@student.ethz.ch
Mrs.	Cassandre	Leverrier		France	cassandre.leverrier@agroparistech.fr
Mrs.	Sandra	Luginbuehl	ETH Zurich	Switzerland	sandra.luginbuehl@mat.ethz.ch
Mr.	Tommaso	Magrini	ETH Zurich	Switzerland	tmagrini@student.ethz.ch
Mr.	Tommaso	Marchesi D'Alvise	EMPA	Switzerland	tommaso.marchesi@empa.ch
Mr.	Michael	Hausmann	EMPA / ETH Zurich	Switzerland	michael.hausmann@mat.ethz.ch
Mr.	Ahmad	Moghimikheirabadi	ETH Zurich	Switzerland	ahmad.moghimikheirabadi@mat.ethz.ch
Mr.	David	Moore	ETH Zurich	Switzerland	david.moore@mat.ethz.ch
Mr.	Chris	Myers	University of Zurich	Switzerland	c.myers@chem.uzh.ch
Dr.	Mathias	Nagel	ETH Zurich	Switzerland	mnagel@mat.ethz.ch
Mrs.	Irene	Natalia	Karlsruhe Institute for Technology	Germany	irene.natalia@kit.edu
Mr.	Francesco	Nazzani	University of Fribourg	Switzerland	francesco.nazzani@unifr.ch
Mr.	Songbo	Ni	ETH Zurich	Switzerland	songbo.ni@mat.ethz.ch

Mrs.	Paola	Orsolini	ETH Zurich / EMPA	Switzerland	paola.orsolini@empa.ch
Mrs.	Elisa M	Ortigosa-Moya	University of Granada	Spain	eortigosa@ugr.es
Dr.	Roberto	Ortuso	University of Geneva	Switzerland	roberto.ortuso@unige.ch
Dr.	Piotr	Owczarz	Lodz University of Technology	Poland	piotr.owczarz@p.lodz.pl
Dr.	Daniel	Palomino	Instrumat AG	Switzerland	daniel.palomino@instrumat.ch
Dr.	Payam	Payamyar	ETH Zurich	Switzerland	ppayam@ethz.ch
Dr.	Christian	Proff	Instrumat AG	Switzerland	christian.proff@instrumat.ch
Dr.	Patrick	Rühs	ETH Zurich	Switzerland	patrick.ruehs@mat.ethz.ch
Dr.	Milad	Radiom	University of Geneva	Switzerland	milad.radiom@unige.ch
Mr.	Steffen	Recktenwald	Karlsruhe Insitute of Technology	Germany	steffen.recktenwald@kit.edu
Mr.	Damian	Renggli	ETH Zurich	Switzerland	damian.renggli@mat.ethz.ch
Dr.	Mathias	Reufer	LS Instruments AG	Switzerland	mathias.reufer@lsinstruments.ch
Mrs.	Sara Tatiana	Roldan Velasquez	ETH Zurich	Switzerland	rosara@student.ethz.ch
Mrs.	Francesca	Ruggeri	University of Zurich	Switzerland	f.ruggeri@pci.uzh.ch
Mrs.	Laura	Scheidegger	ETH Zurich	Switzerland	laursche@student.ethz.ch
Mr.	Bram	Schroyen	ETH Zurich	Switzerland	bram.schroyen@math.ethz.ch
Dr.	Nesrin	Senbil	University of Fribourg	Switzerland	nesrin.senbil@unifr.ch
Dr.	Keshvad	Shahrivar	University of Granada	Spain	kshahrivar@ugr.es
Dr.	Yi	Shen	ETH Zurich	Switzerland	yi.shen@hest.ethz.ch
Mrs.	Katrina	Smith-Mannschott			ksmithmannschott@gmail.com
Mr.	Hendrik	Spanke	ETH Zurich	Switzerland	hspanke@student.ethz.ch
Mr.	Mathias	Steinacher	EPFL	Switzerland	mathias.steinacher@epfl.ch
Prof.	Andre	Studart	ETH Zurich	Switzerland	andre.studart@mat.ethz.ch
Dr.	Wenjie	Sun	ETH Zurich	Switzerland	wenjie.sun@hest.ethz.ch
Prof.	Theo	Tervoort	ETH Zurich	Switzerland	theo.tervoort@mat.ethz.ch
Mr.	Adam	Townsend	University College London	United Kingdom	a.townsend@ucl.ac.uk
Mrs.	Maria	Tsemperouli	University of Geneva	Switzerland	maria.tsemperouli@unige.ch

Mrs.	Merel	van den Berg	ETH Zurich	Switzerland	merel.vandenberg@hest.ethz.ch
Mr.	Siddarth	Vasudevan	ETH Zurich	Switzerland	siddarth.vasudevan@mat.ethz.ch
Dr.	Jan	Vermant	ETH Zurich	Switzerland	jan.vermant@mat.ethz.ch
Dr.	Trappe	Veronique	University of Fribourg	Switzerland	Veronique.Trappe@unifr.ch
Mr.	Antoine	Vian	EPFL	Switzerland	antoine.vian@epfl.ch
Prof.	Peter	Walde	ETH Zurich	Switzerland	peter.walde@mat.ethz.ch
Mr.	Michele	Zanini	ETH Zurich	Switzerland	michele.zanini@mat.ethz.ch
Dr.	Ning	Zhang	Southeast University / ETH Zurich		
Mr.	Patryk	Zolkowski	Lodz University of Technology	Poland	patryk.ziolkowski.89@gmail.com
Prof.	Andreas	Zumbuehl	University of Fribourg	Switzerland	andreas.zumbuehl@unifr.ch